Calcium Dependence of Inactivation of Calcium Release from the Sarcoplasmic Reticulum in Skeletal Muscle Fibers

BRUCE J. SIMON, MICHAEL G. KLEIN, and MARTIN F. SCHNEIDER

From the Department of Biological Chemistry, University of Maryland School of Medicine, Baltimore, Maryland 21201

ABSTRACT The steady-state calcium dependence of inactivation of calcium release from the sarcoplasmic reticulum was studied in voltage-clamped, cut segments of frog skeletal muscle fibers containing two calcium indicators, fura-2 and antipyrylazo III (AP III). Fura-2 fluorescence was used to monitor resting calcium and relatively small calcium transients during small depolarizations. AP III absorbance signals were used to monitor larger calcium transients during larger depolarizations. The rate of release (R_{rel}) of calcium from the sarcoplasmic reticulum was calculated from the calcium transients. The equilibrium calcium dependence of inactivation of calcium release was determined using 200-ms prepulses of various amplitudes to elevate [Ca^{2+}] to various steady levels. Each prepulse was followed by a constant test pulse. The suppression of peak R_{rel} during the test pulse provided a measure of the extent of inactivation of release at the end of the prepulse. The [Ca^{2+}] dependence of inactivation indicated that binding of more than one calcium ion was required to inactivate each release channel. Half-maximal inactivation was produced at a [Ca^{2+}] of ~0.3 μM. Variation of the prepulse duration and amplitude showed that the suppression of peak release was consistent with calcium-dependent inactivation of calcium release but not with calcium depletion. The same calcium dependence of inactivation was obtained using different amplitude test pulses to determine the degree of inactivation. Prepulses that produced near maximal inactivation of release during the following test pulse produced no suppression of intramembrane charge movement during the test pulse, indicating that inactivation occurred at a step beyond the voltage sensor for calcium release. Three alternative set of properties that were assumed for the rapidly equilibrating calcium-binding sites intrinsic to the fibers gave somewhat different R_{rel} records, but gave very similar calcium dependence of inactivation. Thus, equilibrium inactivation of calcium release appears to be produced by rather modest increases in [Ca^{2+}] above the resting level and in a steeply calcium-dependent manner. However, the inactivation develops relatively

Address reprint requests to Dr. Martin F. Schneider, Department of Biological Chemistry, University of Maryland School of Medicine, 660 West Redwood Street, Baltimore, MD 21201.

Dr. Simon's present address is Department of Physiology and Biophysics, F41, University of Texas Medical Branch, Galveston, TX 77550.

J. GEN. PHYSIOL. © The Rockefeller University Press · 0022-1295/91/03/0437/35 $2.00
Volume 97 March 1991 437–471

slowly even during marked elevation of [Ca^{2+}], indicating that a calcium-independent transition appears to occur after the initial calcium-binding step.

INTRODUCTION

Release of calcium from the sarcoplasmic reticulum (SR) in a skeletal muscle fiber is activated by fiber depolarization. The elevated myoplasmic [Ca^{2+}] resulting from the calcium release then imposes a negative feedback on the release system in the form of calcium-dependent inactivation of release (Schneider and Simon, 1988). The net result is that when a 100–200-ms depolarizing pulse is applied to a voltage–clamped fiber, the rate of release (R_{rel}) of calcium from the SR transiently rises to an early peak and then declines toward a much lower level (Baylor, Chandler, and Marshall, 1983; Melzer, Rios, and Schneider, 1984). Although a relatively small and slow component of the decline in release is attributable to depletion of calcium from the SR (Schneider, Simon, and Szucs, 1987), the major part of the early decline in the rate of calcium release in voltage-clamped fibers appears to be due to calcium-dependent inactivation of release (Schneider and Simon, 1988). Evidence for a calcium-dependent suppression of calcium release has also been obtained from skinned skeletal muscle fibers (Kwok and Best, 1987), from SR vesicles isolated from skeletal fibers (Meissner, Darling, and Eveleth, 1986), and from skinned cardiac cells (Fabiato, 1985).

A serious limitation in our previous study of calcium-dependent inactivation of calcium release from the SR in voltage-clamped fibers (Schneider and Simon, 1988) was the inability to monitor resting [Ca^{2+}] because of the relatively low affinity of the calcium indicator antipyrylazo III (AP III) used in those studies. To overcome this limitation, we have recently developed apparatus to use the higher affinity calcium indicator fura-2 (Grynkiewicz, Poenie, and Tsien, 1985) simultaneously with AP III in the same fiber in order to monitor both resting [Ca^{2+}] and the calcium transients elicited by fiber depolarization (Klein, Simon, Szucs, and Schneider, 1988). In the present work we use this apparatus to further investigate the inactivation of calcium release from the SR. Our results are consistent with a calcium-dependent inactivation process that produces half-maximal inactivation at ~0.3 μM [Ca^{2+}], and indicate that more than one calcium-binding site must be occupied in order to inactivate an SR calcium release channel.

Some aspects of this work have been presented in abstract form (Simon, Klein, and Schneider, 1988).

METHODS

Single muscle fibers from the ileofibularis or semitendinous muscles of frogs (*Rana pipiens*, northern variety) were dissected, cut at both ends, and mounted in a double Vaseline gap chamber, all in a relaxing solution (Kovacs, Rios, and Schneider, 1983). Fibers were stretched to 3.8–4.1 μm per sarcomere and notched just beyond the walls in both end pools. After forming Vaseline seals and positioning covering pieces (Kovacs et al., 1983) the solutions in the middle and end pools were changed to those used for the experiments. The "internal" solution applied to the cut ends of the fibers contained (in mM): 102.5 Cs^+ glutamate, 5.5 $MgCl_2$, 5 ATP (disodium salt), 4.5 Na^+ Tris-maleate buffer, 13.2 Cs^+ Tris-maleate buffer, 0.1 EGTA, 5 creatine phosphate (disodium salt), 1 AP III, 0.05 fura-2, and 6 glucose. The "external" solution applied to the intact portion of the fiber in the middle pool contained (in mM): 75

$(TEA)_2SO_4$, 5 Cs_2SO_4, 7.5 total $CaSO_4$, 5 Na^+ Tris-maleate buffer, and 10^{-7} g/ml tetrodotoxin. Both solutions were adjusted to pH 7.0 at room temperature. Fibers were voltage clamped and current and voltage were monitored using standard circuits (Kovacs et al., 1983). Experiments were carried out at a holding potential of −100 mV and at 8–10°C.

Optical absorbance and fluorescence measurements were carried out as described by Klein et al. (1988). Calcium transients $\Delta[Ca^{2+}]$ were calculated from the AP III absorbance signals at 700 nm (Klein et al., 1988) using the calibration of Kovacs et al. (1983). Simultaneously recorded fura-2 fluorescence signals and AP III calcium transients were used to calibrate the fura-2 signals in each fiber so as to be consistent with the $\Delta[Ca^{2+}]$ determined from AP III (Klein et al., 1988). The fura-2 fluorescence signals in the resting fiber were then used with this calibration to calculate resting $[Ca^{2+}]$.

The rate of release (R_{rel}) of calcium from the SR was calculated from each $\Delta[Ca^{2+}]$ according to the general approach of Melzer, Rios, and Schneider (1984, 1987), using method 1 of Melzer et al. (1987). Details regarding the specific myoplasmic calcium-binding sites, both rapidly and slowly equilibrating, used in the present standard calculations of calcium removal and R_{rel} were as described by Klein, Simon, and Schneider (1990). In our standard calculations we assumed the calcium-specific binding sites on thin filament troponin C to be present at 250 μM (referred to myoplasmic water) and to have on and off rate constants of 1.3×10^8 M^{-1} s^{-1} and 10^3 s^{-1}, and assumed the calcium-binding sites on the SR calcium pump to be present at 200 μM. The various values of the calcium removal system parameters were set or adjusted as described by Klein et al. (1990). In a few cases we used alternative assumptions regarding the properties of the calcium pump or the troponin C sites to determine the extent to which our conclusions regarding inactivation might depend on the assumptions regarding the rapidly equilibrating calcium-binding sites intrinsic to the fiber. The alternative parameters will be described in detail in the Results. The on and off rate constants for calcium binding to the troponin C used in our standard calculations give a dissociation constant of 7.7 μM, which is relatively large compared with that reported from other studies (cf. Baylor et al., 1983 for tabulation). We use the higher value so that our removal model can reproduce the close to exponential decline of $\Delta[Ca^{2+}]$ after most calcium transients (Melzer, Rios, and Schneider, 1986*a* and 1987). Use of considerably lower values results in appreciable deviations from simple exponential decline in the $\Delta[Ca^{2+}]$ predicted by the removal model due to saturation of troponin C.

Monitoring, acquisition, processing, and storage of electrical and optical signals were all carried out as described by Klein et al. (1990). Two electrical signals, fiber current and voltage, and three optical signals, fiber light transmission at 700 and 850 nm and fiber fluorescence at 510 nm (excitation at 380 nm), were monitored sequentially at 40-μs intervals during each 200-μs interval. Each point in the stored record for a given signal consisted of the average of 5 or 10 such determinations of that signal over a 1- or 2-ms interval, respectively. For all pulses in which charge movement was monitored the sampling interval was 1 ms per point for each record. Signal averaging of repeated applications of the same pulse was carried out only for experiments in which charge movement was measured.

Currents I_Q due to intramembrane charge movement were determined as described by Melzer, Schneider, Simon, and Szucs (1986*b*). Both before and after each sequence of depolarizing pulses in which charge movement was monitored, the current for a 100-ms, 20-mV hyperpolarization from the holding potential of −100 mV was averaged over 32 pulse applications. After the experiment the "OFF" currents at the end of these two signal-averaged records were averaged. Using this overall average current record, a straight sloping baseline was fit to points 51–100 after the pulse and the resulting straight line was subtracted from the entire OFF segment of the record. The remaining current during the first 50 ms of the OFF segment was assumed to represent the linear capacitative current of the fiber. It was used as the

"control" linear capacitative transient in the calculation of the charge movement current I_Q for each depolarizing pulse in the intervening sequence. Linear capacitative current was removed from the current for each depolarizing pulse by moving the control transient to the start of each step of the depolarizing pulse, scaling it by the step size divided by 20 mV, and subtracting it from the current for the depolarizing pulse. The entire 50-ms control current segment was used in this manner even if the step in the depolarizing pulse lasted <50 ms (Melzer et al., 1986*b*).

Constant and slowly changing ionic currents were removed from the remaining current for each step by fitting a straight, sloping baseline to points 51–100 after the step and then subtracting the line from the entire duration of the step. Any remaining current during the first 50 ms of each step was assumed to be the current due to intramembrane charge movement. The pulse protocol for determining inactivation of calcium release included some steps that lasted only 10 ms, which was too short an interval for determining the ionic current baseline. For such steps, the same step was always applied for 100 ms in another pulse but was still preceded by the identical sequence of steps that preceded the 10-ms step. The first 10 ms of the fully corrected current for the 100-ms step was then used as the charge movement current for the 10-ms step.

Throughout the text average values are given as the mean ± SEM of a variable. Statistical significance was determined using a two-tailed t test assuming significance for $P \leq 0.05$. Fitting of various models to the calcium dependence of inactivation of release was carried out using the generalized data fitting program NFIT (Island Products, Galveston, TX) developed by Dr. Simon.

RESULTS

Inactivation of Peak Release by a Prepulse

Fig. 1 illustrates the basic pulse protocol used to determine the steady-state calcium dependence of inactivation of calcium release from the SR. A constant test pulse, in this case a 100-ms pulse to −20 mV, was applied either by itself or following a 200-ms prepulse to various potentials as indicated at the bottom of Fig. 1. In each case a 10-ms hyperpolarizing pulse to −120 mV directly preceded the test pulse. When a prepulse was applied, the pulse to −120 mV directly followed the prepulse. This brief hyperpolarization was intended to restore the T-tubule (TT) voltage sensor for SR calcium release to the same initial state before the test pulse, independent of the presence or size of the preceding prepulse.

The upper row of Fig. 1 presents the calcium transients resulting from the pulses at the bottom. The first $\Delta[Ca^{2+}]$ record (left) was for the test pulse without any prepulse. For the next three $\Delta[Ca^{2+}]$ records the prepulse voltage was increased successively from −60 to −50 to −45 mV (bottom), causing an increasing elevation of $[Ca^{2+}]$ before the test pulse. For the two smaller prepulses $\Delta[Ca^{2+}]$ was essentially constant during the latter part of the prepulse. For the largest prepulse $\Delta[Ca^{2+}]$ increased very slowly during the latter part of the prepulse. During the 10-ms hyperpolarizing pulse between each pre- and test pulse there was a clear inflection and slight droop in $\Delta[Ca^{2+}]$, indicating the expected turn off of release during hyperpolarization. However, the hyperpolarization was sufficiently brief that the droop in $\Delta[Ca^{2+}]$ between the pre- and test pulses was minimal. As the prepulse was increased in amplitude there was a modest decrease in the peak amplitude of $\Delta[Ca^{2+}]$ during the test pulse.

The second row of Fig. 1 shows the rate of release of calcium from the SR calculated from each of the calcium transients in the upper row. For the test pulse alone (left), R_{rel} reached an early peak and then declined toward a lower level. As previously shown, the major part of the fast decline in release is due to calcium-

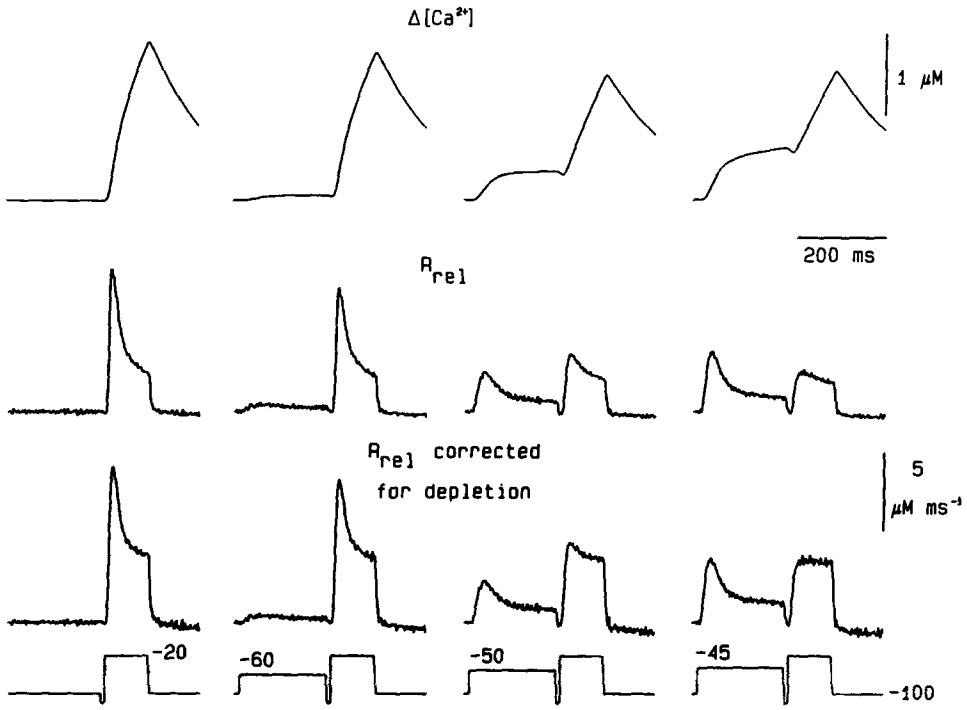

FIGURE 1. Inactivation of the peak component of the rate of release (R_{rel}) by elevated [Ca^{2+}]. *Top row,* Δ[Ca^{2+}] for an 80-mV, 100-ms test depolarization alone (left-most record) or preceded by a 200-ms prepulse to −60, −50, or −45 mV. In all cases, the test pulse was immediately preceded by a 10-ms step to −120 mV. *Second row,* The rate of release of calcium from the SR calculated from the Δ[Ca^{2+}] records above, uncorrected for the effects of Ca^{2+} depletion from the SR. *Third row,* The rate of release corrected for depletion of [Ca^{2+}] from the SR, assuming that the SR calcium content at the beginning of each record gives 1.1 mM [Ca^{2+}] if dissolved in myoplasmic water. The pulse protocol is shown at the bottom. The R_{rel} was calculated after characterizing the [Ca^{2+}] removal properties of the fiber by a least-squares fit to the decay of Δ[Ca^{2+}] after the test pulse (see text). The best-fitting values were $k_{off,Mg\text{-}Parv}$ = 4.1 s^{-1}, SR calcium pump V_{max} = 362 μM s^{-1}, and the total concentration ([Parv]) of Ca^{2+}/Mg^{2+} sites on parvalbumin = 711 μM. Fiber 492, AP III concentration 1,364–1,597 μM, resting [Ca^{2+}] 28–40 nM, sarcomere length 4.0 μm, temperature 9°C.

dependent inactivation of release (Schneider et al., 1987; Schneider and Simon, 1988). Consistent with this interpretation, increasing elevations of [Ca^{2+}] before the test pulse due to increasingly larger prepulses (left to right in Fig. 1) increasingly suppressed the early peak in the test pulse release, presumably because of increasing inactivation during the prepulse (Schneider and Simon, 1988). The observation that

release never declined to zero during any pulse, even with the relatively large calcium transients during the largest test pulses (Melzer et al., 1984), indicates that the inactivation of release was never complete (Schneider and Simon, 1988). Only the peak release during the early part of the test pulses in Fig. 1, but not the maintained release later in the test pulse, could be inactivated by a prepulse. A repeat application of the test pulse alone without prepulse (not shown) after applying the prepulses shown in Fig. 1 gave a R_{rel} record essentially identical to the one without prepulse in Fig. 1, indicating negligible fiber run down during the experiment of Fig. 1.

The third row of records in Fig. 1 gives R_{rel} corrected for the decline in release due to depletion of calcium from the SR (Schneider et al., 1987). The depletion correction was carried out assuming that the initial calcium content of the SR before each pulse in this fiber corresponded to a myoplasmic concentration of 1.1 mM if the entire SR calcium content were dissolved in myoplasmic water. The value of the SR calcium content was chosen so that the depletion correction eliminated the slow phase of decline in release records (not shown) for longer pulses to −20 mV (Schneider et al., 1987; Schneider, Simon, and Klein, 1989). After correction for depletion, the final level of R_{rel} at the end of each test pulse in Fig. 1 was essentially the same in all records. This is consistent with the expectation that $[Ca^{2+}]$-dependent inactivation would be maximal by the end of each of the test pulses because of the relatively large test pulse $\Delta[Ca^{2+}]$. The remaining steady release during the latter part of each test pulse corresponds to the component of release that could not be inactivated.

The corrected R_{rel} records in the third row of Fig. 1 show that the largest prepulse (right) completely eliminated the peak in the release record for the following test pulse. Complete suppression of the peak test release occurred even though the amplitudes of both the peak and steady level of release during the prepulse (right) were less than half the respective amplitudes of the peak and steady level of release during the test pulse applied alone (left). Thus, the peak in a test pulse release record could be completely eliminated by a prepulse that produced less than half of the peak or steady activation of release that occurred during the test pulse by itself. Using larger test pulses it was observed that prepulses that produced $<25\%$ of the peak and steady release produced by the test pulse alone could completely eliminate the peak in the test pulse R_{rel} record (below).

The extent of inactivation of release before each test pulse in Fig. 1 can be quantitated using the expression $P/S - 1$, where P is the peak value of R_{rel} during the test pulse and S is the steady value of R_{rel} at the end of the test pulse. This expression gives the relative excess of peak release over steady release during each test pulse and provides a convenient relative measure of the release that could be inactivated but was not inactivated before a particular test pulse. If the peak of the test release were completely suppressed after a prepulse, corresponding to maximum inactivation by the prepulse, and if activation were complete at the time of the peak of release, P/S would equal 1 and $P/S - 1$ would equal zero. However, even though $P/S - 1$ could go to zero, indicating that the peak value of release was the same as the steady value, release was never completely inactivated in our experiments since S was never zero.

The data points in Fig. 2 present $P/S - 1$ for the test pulse segment of each of the depletion-corrected records from Fig. 1 and for four other records from the same

fiber not shown in Fig. 1. $P/S - 1$ is plotted in Fig. 2 as a function of the value of $[Ca^{2+}]$ (log scale) at the end of the prepulse, obtained from the sum of the resting $[Ca^{2+}]$ recorded with fura-2 before the prepulse and the value of $\Delta[Ca^{2+}]$ recorded with AP III at the end of the prepulse. For test pulses without prepulse depolarizations, the appropriate $[Ca^{2+}]$ value was the resting $[Ca^{2+}]$ before the test pulse. This treatment implicitly assumes that calcium binding to the sites responsible for producing inactivation had reached equilibrium by the end of the prepulse. This assumption was confirmed by experiments described below. The data in Fig. 2 indicate that the suppression of peak release developed relatively steeply with

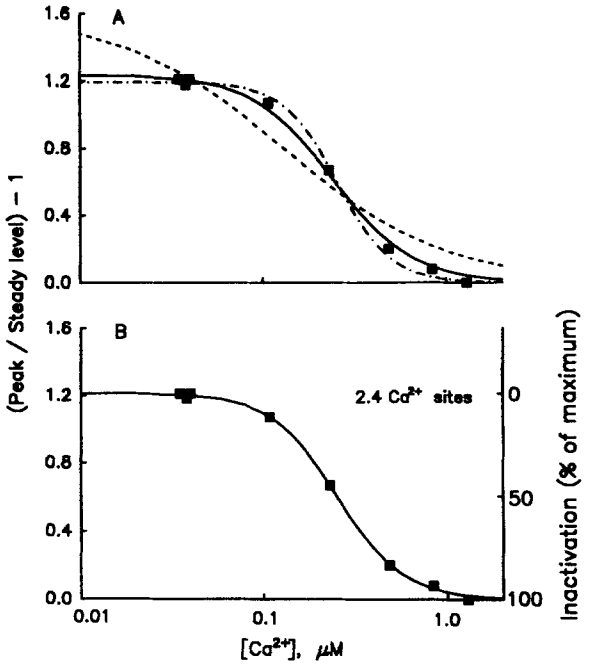

FIGURE 2. The Ca^{2+} dependence of inactivation of the peak R_{rel}. (*A*) The symbols represent the (peak/steady level) − 1 from the depletion-corrected records shown in Fig. 1 and for four other records not shown in that figure, versus the resting $[Ca^{2+}]$ plus the $\Delta[Ca^{2+}]$ measured at the end of the 200-ms prepulse (see text). The abscissa is shown here and hereafter on a logarithmic scale. The theoretical curves are the least-squares fit of Eq. 6 to the data for fixed values of n (the minimum number of Ca^{2+} sites that must be occupied to produce inactivation) with n equal to 1 (*dashed*), 2 (*solid*), and 3 (*dot-dashed*). The best-fitting values were: $Ca_{50} = 0.13$ μM, $f_P/K_S = 1.51$ (*dashed*); $Ca_{50} = 0.24$ μM, $f_P/K_S = 1.22$ (*solid*); and $Ca_{50} = 0.55$ μM, $f_P/K_S = 1.17$ (*dot-dashed*). (*B*) The same data as in *A*, with the solid line representing a least-squares fit of Eq. 6, now allowing n to be varied. The best-fitting values were $Ca_{50} = 0.25$ μM, $f_P/K_S = 1.21$, and $n = 2.41$. The right ordinate gives the percentage of the inactivatable release that was inactivated.

increasing prepulse $[Ca^{2+}]$. Suppression of peak release was half maximal for a prepulse elevation of $[Ca^{2+}]$ to ~0.3 μM and was near maximal for $[Ca^{2+}]$ of ~1 μM. The data in Fig. 2 and similar data from other fibers and fits to these data using a calcium-binding model (below) indicate that at the $[Ca^{2+}]$ levels in resting fibers the suppression of peak release was minimal and relatively independent of $[Ca^{2+}]$.

In order to interpret quantitatively the calcium dependence of $P/S - 1$ in Fig. 2, it is necessary to develop a general formalism for activation and inactivation of release during the pre- and test pulses for the pulse protocol in Figs. 1 and 2 and to consider a specific model for the calcium dependence of inactivation.

General Formalism for Activation and Inactivation of Release in the Prepulse Protocol

A first step in interpreting the suppression of peak test pulse release by prepulse [Ca^{2+}] is to consider how the degree of inactivation at the end of the prepulse is reflected in the test pulse release record. To do this it is convenient to develop a general formalism for activation and inactivation of release. One question that arises immediately in developing such a formalism is the origin of the noninactivatable component of release. Two alternative possibilities that account for the observed R_{rel} waveform, including the noninactivatable component, are (*a*) a uniform population of a single type of SR calcium release channel that exhibits incomplete inactivation, or (*b*) two different types of channels, an inactivating type that gives rise to the decline in release during a pulse and a noninactivating type that gives rise to the steady release. Previous results indicate that if there are two types of channels, they exhibit very similar activation time courses (Simon and Schneider, 1988) and voltage dependence (Melzer et al., 1984; Klein et al., 1990). Although there is no compelling evidence that rules out the presence of two types of channels with these properties, for simplicity we will first interpret our results in terms of only a single type of channel. Some alternative interpretations in terms of two types of channels will be considered in the Discussion. Another question is the relationship between activation and inactivation. If each SR calcium release channel that can undergo inactivation is first activated by the TT voltage sensor but is inactivated by a calcium-dependent process, it seems reasonable to use a formalism in which the mechanisms for activation and inactivation can be treated as separate processes acting in parallel.

Assuming a uniform population of a single type of SR calcium release channel, with each channel having parallel activation and inactivation mechanisms, the rate of calcium release from the SR can be expressed as the product of three terms: an amplitude factor, an activation factor, and an inactivation factor. The amplitude factor would depend on the total number of release channels, the single channel conductance, and the driving force for calcium efflux from the SR. For a uniform population of a single type of channel and for depletion-corrected release records, the amplitude factor would be constant. The activation factor would give the fraction of channels that are activated and the inactivation factor would give the fraction of channels that are not inactivated. Setting the rate of release proportional to the product of the activation and inactivation factors corresponds to the condition that only channels that are both activated and not inactivated are open. The activation factor, denoted by a, could range from 0 to 1 for zero to full activation. The inactivation factor, denoted by b, could in principle range from 1 to 0 for zero to full inactivation. However, in practice inactivation was never observed to be complete in our experiments. Thus, b ranged from 1 to b_{min}, where b_{min} is a minimum value of b corresponding to maximal inactivation.

The preceding formalism can now be used to obtain a relationship between the peak (P) and steady level (S) of a test pulse release record. If $\Delta[Ca^{2+}]$ during the test pulse were sufficiently large so as to produce maximal inactivation by the end of the test pulse, b would equal b_{min} during the steady level of the test release. Under this

condition,

$$P/S - 1 = (a_P b_P/a_S - b_{min})/b_{min} \quad (1)$$

where a_P and b_P are the values of the activation and inactivation factors at the time of peak of the test release and a_S is the value of the activation factor during the steady level of the test release.

In the simplest case, if activation had attained its steady level by the time of peak release, and if there were no change in inactivation between the end of the prepulse and the peak of the test release, a_P would equal a_S and b_P would equal b_{pre}, the value of b at the end of the prepulse. In this case $P/S - 1$ would equal $(b_{pre} - b_{min})/b_{min}$, which directly provides a measure of the relative degree of inactivation at the end of the prepulse. However, inactivation was likely to have increased between the end of the prepulse and the peak of the test release. Thus, in order to use Eq. 1 to determine the extent of inactivation at the end of the prepulse it is necessary to express $P/S - 1$ as a function of the value of the inactivation factor at the end of the prepulse (b_{pre}) rather than the value at peak release (b_P). To do this we define a correction factor f_P as $(a_P b_P/a_S - b_{min})/(b_{pre} - b_{min})$, which when used in Eq. 1 gives

$$P/S - 1 = f_P(b_{pre} - b_{min})/b_{min} \quad (2)$$

If activation during the peak of the test pulse had already attained its steady level, a_P would equal a_S and f_P would equal $(b_P - b_{min})/(b_{pre} - b_{min})$. This is the fraction of the inactivatable release remaining at the end of the prepulse that was still not inactivated at the peak of the test release. If a_P were less than a_S, f_P would be smaller. Assuming the value of f_P to be the same for test pulses after all prepulses in a given pulse sequence, f_P would be a constant scale factor in Eq. 2. The validity of assuming f_P to be constant will be considered below.

A Model for Inactivation Based on Binding of Multiple Calcium Ions

In order to use Eq. 2 to interpret the calcium dependence of inactivation we must next select a specific model that specifies the relationship between $[Ca^{2+}]$ and b. We have previously presented a three-state model for inactivation of calcium release based on calcium binding (Schneider and Simon, 1988). In that model calcium equilibrated rapidly with a single calcium-binding receptor on the SR calcium release channel. The rapid calcium-binding step was followed by a slower conformational change of the calcium receptor complex to a modified conformation corresponding to the inactivated state of the channel (Schneider and Simon, 1988). A model with at least one additional transition beyond the binding step was necessary to account for the observation that for intermediate and large calcium transients the rate of development and extent of inactivation were independent of $[Ca^{2+}]$ (Melzer et al., 1984; Schneider and Simon, 1988).

In the present case we generalize the previous model so as to include rapidly equilibrating, simultaneous binding of n calcium ions to the receptor R to give Ca_nR, followed by a slower transition of Ca_nR to the inactivated state Ca_nR^*:

$$nCa + R \overset{K_F}{\longleftrightarrow} Ca_nR \overset{K_S}{\longrightarrow} Ca_nR^*$$

Scheme 1

Using R, Ca_nR, and Ca_nR^* to represent the fractional concentrations of each of the three states of the receptor, Ca_nR^* gives the fraction of inactivated channels and $1 - Ca_nR^*$ gives the fraction of noninactivated channels. The dissociation constants K_F and K_S for the rapidly and slowly equilibrating steps are given by $R[Ca^{2+}]^n/Ca_nR$ and Ca_nR/Ca_nR^*, respectively.

The fraction b of noninactivated channels is given by

$$b = 1 - Ca_nR^* \tag{3}$$

The equilibrium value of b, b_{eq}, is given by

$$b_{eq} = (K_S[Ca^{2+}]^n + K_FK_S)/[(1 + K_S)[Ca^{2+}]^n + K_FK_S] \tag{4}$$

At zero $[Ca^{2+}]$, b_{eq} equals 1. At saturating $[Ca^{2+}]$, b_{eq} goes to its minimum value, b_{min}, which is given by

$$b_{min} = K_S/(1 + K_S). \tag{5}$$

Using the specific calcium-binding model presented in this section, and assuming inactivation to have reached equilibrium at the end of the prepulses, Eqs. 4 and 5 can be substituted for b_{pre} and b_{min} in Eq. 2 to give

$$P/S - 1 = (f_P/K_S)K'/(K' + [Ca^{2+}]^n) \tag{6}$$

where K' is equal to $K_FK_S/(1 + K_S)$ and $[Ca^{2+}]$ is the free calcium concentration at the end of the prepulse. The $[Ca^{2+}]$ for 50% inactivation, Ca_{50}, is given by the n^{th} root of K'.

Calcium Dependence of Inactivation of Peak Rate of Release

The theoretical lines in Fig. 2 *A* are the best fits to the data using Eq. 6 with n set equal to 1 (dashed), 2 (solid), or 3 (dot-dashed), and with f_P/K_S and K' varied so as to produce the least-squares fit. For each fit f_P was assumed to be the same for all prepulses. The data points in Fig. 2 *A* are poorly fit using $n = 1$ and lie between the fits using $n = 2$ and $n = 3$. In Fig. 2 *B* the same data were fit by Eq. 6, but now we allowed n as well as f_P/K_S and K' to vary as a fit parameter. The theoretical line in Fig. 2 *B*, which uses the best-fit value of 2.4 for n, closely reproduces the observed calcium dependence of suppression of peak release. The calcium dependence of $P/S - 1$ in Fig. 2 thus indicates that at least two calcium ions must be bound to produce inactivation of the SR calcium release channel.

Values of n obtained from fits of Eq. 6 to data similar to that in Fig. 2 from 10 fibers are presented in Table I. The fits were carried out adjusting n, f_P/K_S, and K' to produce a best fit. In all cases n was found to be > 1 and < 4. The mean ± SEM value of n was 1.87 ± 0.22. Thus, the conclusion that more than one calcium ion must bind in order to produce inactivation applies to all fibers studied. Table I also presents values of Ca_{50}, the $[Ca^{2+}]$ for 50% inactivation, obtained from the fits to the data from each fiber. Ca_{50} ranged from 0.13 to 0.66 μM, with a mean value of 0.34 ± 0.05 μM.

The last column of Table I gives the value of the fura-2 calcium dissociation constant (K_D) obtained in each fiber by adjusting the fura-2 parameters so as to force the fura-2 record to be consistent with the simultaneously recorded AP III calcium transient (Klein et al., 1988). Since the calcium transient calculated from the AP III

signal may underestimate the true calcium transient by a factor that could be as large as seven to nine due to binding of AP III to myoplasmic constituents (Baylor, Hollingworth, Hui, and Quinta-Ferreira, 1986; Maylie, Irving, Sizto, and Chandler, 1987; Hirota, Chandler, Southwick, and Waggoner, 1989), the values given in Table I for the fura-2 K_D and the Ca_{50} in each fiber would be underestimated by the same percentage as the underestimate of the AP III calcium transient.

As $[Ca^{2+}]$ approaches zero the expression for $P/S - 1$ in Eq. 6 approaches f_P/K_S. Thus, the low $[Ca^{2+}]$ values of $P/S - 1$ potentially provide a means of estimating f_P/K_S. The fit to the data in Fig. 2 *B* and similar fits to data from the other fibers in Table I indicate that the value of $P/S - 1$ at resting $[Ca^{2+}]$ was close to the limiting value that would be obtained at zero $[Ca^{2+}]$. The fourth column of Table I presents the values of f_P/K_S obtained from the fits of Eq. 6. For the 10 fibers in Table I the mean value of f_P/K_S obtained from the fit parameters was 2.77 ± 0.36.

TABLE I

The $[Ca^{2+}]$ Dependence of Inactivation of R_{ml}

Fiber reference	Ca_{50}	n	f_P/K_S	fura-2 K_D
	μM			μM
409	0.66	1.73	1.75	189
436	0.31	1.45	1.56	73
456	0.52	3.60	2.00	64
475	0.30	1.47	4.54	55
477	0.47	1.79	3.80	69
478	0.21	1.66	3.10	74
479	0.31	1.62	2.96	60
481	0.23	1.48	3.16	101
492	0.25	2.41	1.21	65
503	0.13	1.48	3.66	59
Mean ± SEM	0.34 ± 0.05	1.87 ± 0.22	2.77 ± 0.36	81 ± 13

Ca_{50} is the $[Ca^{2+}]$ for 50% inactivation of R_{ml}, n is the minimum number of sites that must be occupied by Ca^{2+} to produce inactivation, f_P/K_S is the limiting value of $P/S - 1$ evaluated at zero $[Ca^{2+}]$ (see text). K_D is the dissociation constant for Ca-fura-2.

The value of f_P depends on the degree of inactivation before the test pulse and on the kinetics of development of activation and inactivation during the test pulse. For test pulses without prepulses inactivation was negligible before the pulse (above), so only the activation and inactivation time courses need be determined to estimate f_P. These can be estimated by making a correction based on the observed exponential time course of inactivation late during the test pulse when activation should have been constant (Simon and Schneider, 1988). Using the rough approximation that the inactivation factor b remained equal to 1 until $[Ca^{2+}]$ reached Ca_{50}, and then changed exponentially from 1 to b_{min} with the time constant observed late in the pulse, values of f_P were obtained for each of the sequences in Table I. The mean value obtained for f_P was 0.35 ± 0.5. Using this value with the mean value of f_P/K_S from Table I, the value of K_S would be 0.13, which, from the definition of K_S, is the equilibrium value of

Ca_nR/Ca_nR^*. With this value of K_S, 11% of the channels would remain noninactivated at sufficiently high $[Ca^{2+}]$ to produce calcium binding to all inactivation sites.

The preceding analysis of the calcium dependence of inactivation was based on the assumption that the value of the factor f_P was the same for all prepulses used to elevate $[Ca^{2+}]$. We also carried out an alternative analysis that involved somewhat different assumptions. Rearranging Eq. 1 as

$$a_SP/a_PS - 1 = (b_P - b_{min})/b_{min} \tag{7}$$

provides an equation that contains only inactivation factors on the right side. Defining a new correction factor g_P as $(b_P - b_{min})/(b_{pre} - b_{min})$, Eq. 7 can be expressed in terms of b_{pre} rather than b_P,

$$a_SP/a_PS - 1 = g_P(b_{pre} - b_{min})/b_{min} \tag{8}$$

The correction factor g_P is analogous to f_P, but in contrast to f_P it contains only inactivation factors and is independent of the activation factors. Using the model in Scheme 1, Eqs. 4 and 5 can again be used for b_{pre} and b_{min} to give

$$a_SP/a_PS - 1 = (g_P/K_S)K'/(K' + [Ca^{2+}]^n) \tag{9}$$

The left side of Eq. 9 contains not only the parameters P and S that are obtained directly from the release records, but also the activation factors a_P and a_S. However, it is possible to obtain an estimate of the time course of activation during each test pulse by correcting the observed rate of release for inactivation as previously described (Simon and Schneider, 1988). The activation time course can then be used to obtain a value for a_S/a_P for each test pulse. We have used this procedure to evaluate $a_SP/a_PS - 1$ for each of the test pulses in each of the inactivation runs in Table I. The resulting data from each fiber were fit by Eq. 9, assuming g_P to be constant. Excluding one fiber in which the resulting data exhibited too much scatter for the fit to converge, the mean value of n obtained from the fits was 1.99 ± 0.24 ($n = 9$), which is not significantly different from the mean value of 1.87 ± 0.22 ($n = 10$) in Table I ($P > 0.5$). Thus the assumption that g_P is constant in the fits to $a_SP/a_PS - 1$ results in essentially the same value of n as the assumption that f_P is constant in the fits to $P/S - 1$. Since inactivation is likely to progress from b_{pre} to b_{min} with the same time constant during each test pulse once $[Ca^{2+}]$ is elevated (Melzer et al., 1984), the assumption of constant g_P for test pulses after each prepulse does not seem to be unreasonable.

An equation identical in form to Eq. 9 can also be obtained for the case of two classes of SR calcium release channels, one completely inactivating and the other noninactivating (see Discussion). Thus, the values of n and Ca_{50} obtained from the fits of Eq. 9 could also apply to SR calcium release channels exhibiting complete calcium-dependent inactivation.

Inactivation Had Reached Equilibrium by the End of the 200-ms Prepulses

The theoretical curves in Fig. 2 were calculated assuming that the elevation of $[Ca^{2+}]$ during each prepulse was sufficiently prolonged and sufficiently constant that calcium binding to any sites responsible for producing calcium-dependent inactivation would have reached equilibrium by the end of the prepulse. The experiment in Fig. 3 was designed to test these assumptions and also to verify that depletion of calcium from

the SR was not a factor in producing the fast decline in release that we attribute to calcium-dependent inactivation. The pulse protocol for this experiment (Fig. 3, bottom) again was a constant test pulse, here a 100-ms pulse to −20 mV, either applied alone (left- and right-most panels) or preceded by a prepulse, in the case of Fig. 3 to −40 mV (middle panels). In contrast to the experiments of Figs. 1 and 2, where a constant duration was used for all prepulses, in Fig. 3 the duration of the prepulses was varied, using 100 ms for the prepulse on the left and 400 ms for the

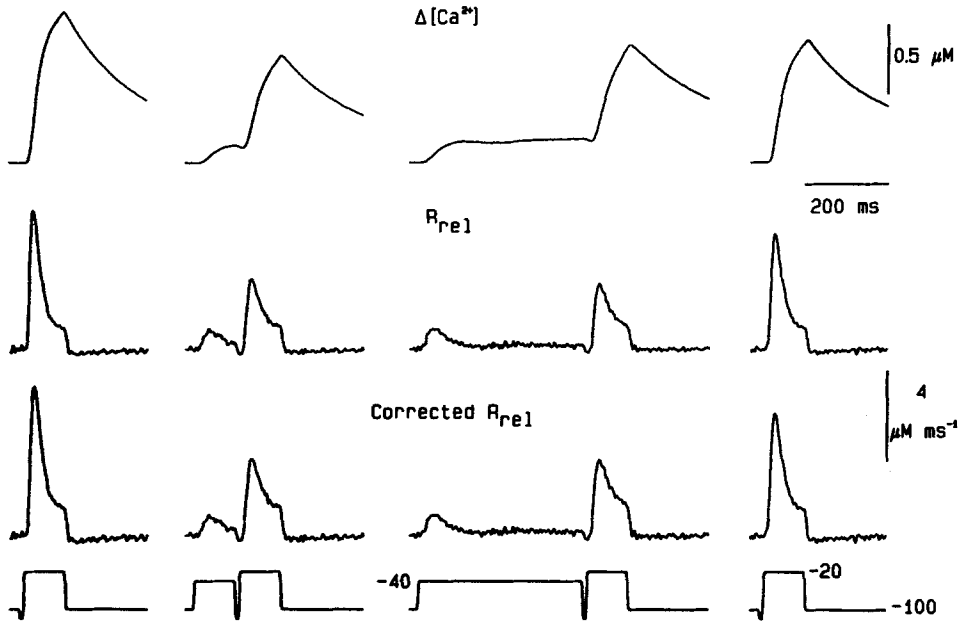

FIGURE 3. The effect of prepulse duration on the inactivation of R_{rel} at constant [Ca^{2+}]. *Top row,* Δ[Ca^{2+}] for an 80-mV, 100-ms test depolarization alone (bracketing controls, left- and right-most records), or preceded by a prepulse to −40 mV of 100 ms (second record from left) or 400 ms (third from left). *Second row,* R_{rel} calculated from the Δ[Ca^{2+}] records above. *Third row,* Corresponding R_{rel} records corrected for Ca^{2+} depletion from the SR, assuming an initial SR Ca^{2+} content of 1.0 mM. The pulse protocol is shown at the bottom. The removal model parameters were $k_{off,Mg\text{-}Parv}$ = 1.2 s^{-1} and pump V_{max} = 528 μM s^{-1}. [Parv] was set to 300 μM. Fiber 488, [AP III] 1,202–1,386 μM, resting [Ca^{2+}] 33–49 nM, 3.9 μm per sarcomere, temperature 8°C.

prepulse on the right. Here, as in the experiment in Fig. 1 and in all other experiments in this paper, a 10-ms hyperpolarization to −120 mV was used to reset the voltage sensor before each test pulse. This brief hyperpolarization caused little change in [Ca^{2+}] between the end of a prepulse and the start of the test pulse.

The calcium transients in the upper row of Fig. 3 illustrate the effect of prolonging the prepulses on Δ[Ca^{2+}]. During the shorter (100-ms) prepulse Δ[Ca^{2+}] rose gradually but became approximately steady by the end of the prepulse. For the

longer (400-ms) prepulse $\Delta[Ca^{2+}]$ was maintained at about the level reached at the end of the 100-ms prepulse, but for an additional 300 ms. Thus, if the elevation of $[Ca^{2+}]$ during the shorter prepulse were not sufficiently prolonged to reach equilibrium for calcium-dependent inactivation, the suppression of peak release during the test pulse following the longer prepulse should have been greater than for the shorter prepulse. The release records (Fig. 3, second row of records) calculated from each of the calcium transients indicate that this was not the case. Suppression of peak release was approximately the same for the test pulse after both the 100- and 400-ms prepulses. The third row of records in Fig. 3 presents release corrected for depletion

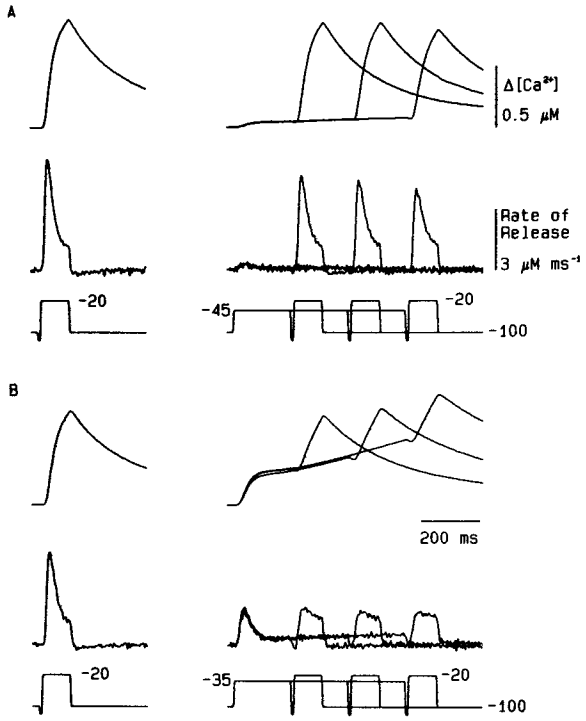

FIGURE 4. The effect of prepulse duration on the inactivation of R_{rel}. (*A*) *Top row*, $\Delta[Ca^{2+}]$ for a test pulse alone (*left*) and for a test pulse preceded by a prepulse to −45 mV for 200, 400, and 600 ms (superimposed, *right*). *Second row*, R_{rel} calculated from the corresponding $[Ca^{2+}]$ records above, corrected for SR Ca^{2+} depletion. The pulse protocol is shown at the bottom. (*B*) Same format as *A*, with a prepulse to −35 mV. The calibration bars apply to both *A* and *B*. Same fiber and conditions as in Fig. 3.

of calcium from the SR. These records exhibit essentially the same features as the uncorrected release records in the second row.

The records for the test pulses without prepulses in Fig. 3 constitute bracketing controls that were applied some time before (left column) and some time after (right column) the pulses for the middle two columns in Fig. 3. Comparison of the bracketing controls indicates that the peak rate of release declined slowly over the course of the experiment, but that the steady level of release did not. This behavior is typical of the run down of release that is observed over the course of some experiments (Klein et al., 1990). The run down of release must be taken into account when examining the basis for the suppression of $P/S - 1$ in this experiment (below). The run down of peak release for the test pulses without prepulses in Fig. 3 does not

seem to be due to an increase in inactivation due to an elevation of resting $[Ca^{2+}]$, which was 33 and 40 nM for the left and right columns in Fig. 3, since inactivation was essentially independent of $[Ca^{2+}]$ over this range (above).

Fig. 4 (right) presents superimposed calcium transients and release records from the same fiber as Fig. 3, but for 200-, 400-, and 600-ms prepulses to −45 mV (*A*) or −35 mV (*B*). Records for the test pulse applied without prepulse at about the same time during the experiment as the superimposed records are presented on the left. $\Delta[Ca^{2+}]$ during the prepulse to −45 mV (Fig. 4 *A*) was smaller than during the prepulse to −40 mV in Fig. 3 and produced less suppression of release. In contrast, the prepulse to −35 mV (Fig. 4 *B*) produced a larger $\Delta[Ca^{2+}]$ that slowly increased throughout the prepulse. Consistent with the expectation for calcium-dependent inactivation, this prepulse produced a larger suppression of release and the suppression increased with increasing pulse duration, resulting in almost complete elimination of the peak in the test pulse release after the 200-ms prepulse to −35 mV. The

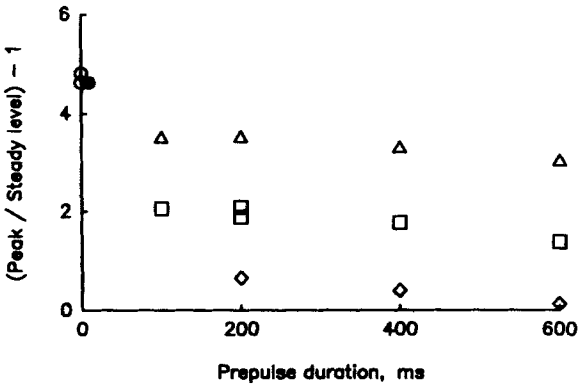

FIGURE 5. The dependence of (peak/steady level) − 1 on prepulse duration, from the experiments shown in Figs. 3 and 4. Different symbols represent different prepulse amplitudes in this figure and in Figs. 6 and 7. *Circles,* No prepulse; *triangles,* prepulse to −45 mV; *squares,* prepulse to −40 mV; *diamonds,* prepulse to −35 mV. The data have been corrected for run down of the peak R_{rel} (see text), which is evident when comparing the records without a prepulse in Figs. 3 and 4. The filled circle represents a final measurement whose value was forced to equal the first measured point. It has been shifted slightly along the abscissa for clarity.

small progressive decrease in peak release with increasing pulse duration in Fig. 4 *A* was largely due to slow run down of peak release over the course of the experiment.

Fig. 5 presents the relative suppression of peak test pulse R_{rel} as a function of prepulse duration for the records in Figs. 3 and 4, and for several other records from the same fiber (not shown). The different symbols in Fig. 5 denote prepulses to −45 mV (triangles), −40 mV (squares), or −35 mV (diamonds), or no prepulse at all (circles). The values of $P/S - 1$ presented in Fig. 5 have been corrected for the run down of peak release seen with test pulses applied at various times during the experiment without any prepulse (Fig. 3). The correction factor for each pulse was calculated from the values of $P/S - 1$ obtained for test pulses applied by themselves at the start and end of the experiment, assuming $P/S - 1$ to decline linearly with time over the course of the experiment. The filled circle denotes the corrected value of $P/S - 1$ for the test pulse applied alone at the end of the experiment, which was forced by the correction procedure to equal the value for the test pulse by itself at the

start of the run, but is plotted at the resting [Ca^{2+}] at the end of the run. The uncorrected value of $P/S - 1$ for this pulse was 3.0. The third circle in Fig. 5 is the corrected value of $P/S - 1$ for another test pulse applied by itself near the middle of the experiment. Its close agreement with the two points used in the correction for run down indicates that the correction was adequate. Values of $P/S - 1$ for all prepulses were corrected for run down using the correction factors obtained from the change of peak R_{rel} in the test pulses applied by themselves at the start and end of the experiment, again assuming linear decline over the course of the experiment.

Suppression of Peak Release Is Consistent with Calcium Binding but Not with Calcium Depletion

Fig. 6 examines the hypothesis that the suppression of release in the experiment of Figs. 3–5 was due to calcium-dependent inactivation. The values of $P/S - 1$ from Fig. 5 are presented again in Fig. 6, but now as a function of the level of [Ca^{2+}] at the end of the prepulse. The various symbols in Fig. 6 denote the same prepulse voltages as

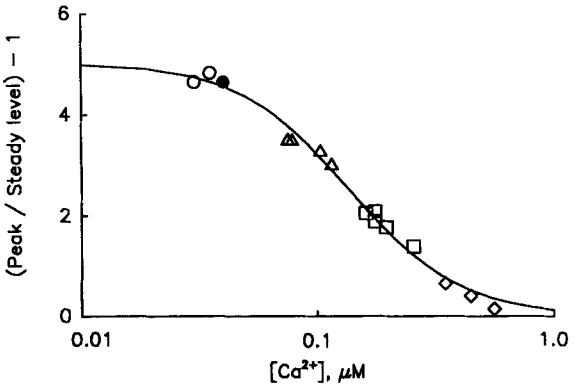

FIGURE 6. The [Ca^{2+}] dependence of (peak/steady level) − 1, from the experiments of Figs. 3 and 4. [Ca^{2+}] at the end of the prepulse was determined in the usual way. Different symbols have the same significance as in Fig. 5. The solid line is a least-squares fit of Eq. 6 to the data with Ca_{50} = 0.14 μM, f_P/K_S = 4.88, and n = 1.85.

in Fig. 5. The line in Fig. 6 gives the best fit of the calcium-binding relationship (Eq. 6) to the data. The relative suppression of peak R_{rel} during test pulses after prepulses of all amplitudes and durations is clearly very well accounted for on the basis of the same equilibrium relationship for inactivation due to calcium binding. The values of Ca_{50} and n derived from the fit were 0.14 μM and 1.85, respectively.

Fig. 7 examines an alternative hypothesis for the cause of the suppression of peak release during the test pulses; namely, that the suppression was due to depletion of calcium from the SR during the prepulse. Previous results have indicated that the relatively slow decline in release seen late after the peak release during depolarizing pulses is due to calcium depletion (Schneider et al., 1987), and the release records in Figs. 3 and 4 have already been corrected for this slow decline due to depletion. We are now considering whether the relatively fast decline in release and the suppression of release by prepulses that elevate [Ca^{2+}] could also be due to depletion of calcium from the SR. In this case the suppression of peak release should be determined by the amount of calcium released from the SR during the prepulse, which can be calculated directly as the integral of the uncorrected R_{rel}. To test this hypothesis the

values of $P/S - 1$ from Figs. 5 and 6 are plotted in Fig. 7 as a function of the amount of calcium released from the SR during the prepulse. As in the preceding figures, each symbol denotes a different prepulse voltage. A straight line was drawn by eye through the values for each prepulse voltage. If depletion were the cause of the decline in $P/S - 1$, different amplitude and duration prepulses that released about the same amount of calcium should have produced about the same degree of suppression of peak release. Fig. 7 indicates that this was not the case. For each group of points (indicated by different symbols) where two different amplitude prepulses released similar amounts of calcium, the larger prepulses systematically produced greater suppression of $P/S - 1$. This is inconsistent with depletion causing the suppression of release but is consistent with calcium-dependent inactivation producing the suppression (Fig. 6) since the larger prepulses produced a greater elevation of $[Ca^{2+}]$. Results similar to those in Figs. 6 and 7 were obtained from the one other fiber in which the effects of different duration prepulses were examined.

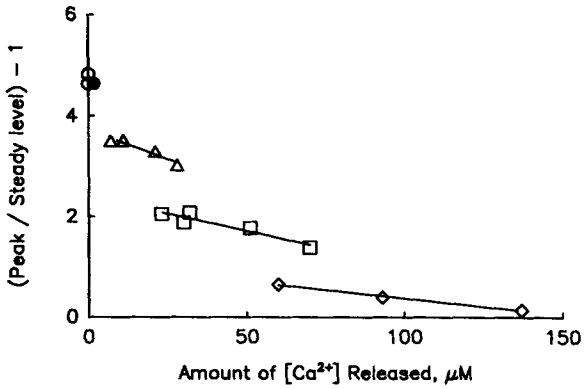

FIGURE 7. The dependence of (peak/steady level) − 1 on the amount of Ca^{2+} released during the prepulse from the experiments shown in Figs. 3 and 4. The amount of released Ca^{2+} was calculated as the running integral of the R_{rel} during the prepulse. The different symbols indicate different prepulse voltages as in Fig. 5. Straight lines drawn by eye.

The Calcium Dependence of Inactivation Is the Same for Different Amplitude Test Pulses

If the suppression of peak release at the end of a prepulse is due to calcium binding to sites that produce inactivation by a mechanism that is independent of the activation process, the extent of inactivation should be the same for test pulses that produce different degrees of activation. Fig. 8 presents records from an experiment designed to test whether the calcium dependence of inactivation was the same when different amplitude test pulses were used to determine the extent of inactivation. Both *A* and *B* of Fig. 8 present $\Delta[Ca^{2+}]$ (top row of records in each part), R_{rel} (second row), and R_{rel} corrected for depletion (third row) for an 80-ms test pulse applied alone (left) and for the test pulse preceded by a 200-ms prepulse to −40, −35, or −30 mV, as indicated by the voltage traces at the bottom of *A* and *B*. The only difference in the pulse protocols in *A* and *B* was that the test pulse was to −20 mV in *A* and to +20 mV in *B*. The prepulse segments of the $\Delta[Ca^{2+}]$ and release records were thus essentially the same for a given column in Fig. 8. In contrast, the test pulse

segments of the $\Delta[Ca^{2+}]$ and release records were considerably larger for the larger test pulse (Fig. 8 *B*) than for the smaller test pulse (Fig. 8 *A*). Because of the larger release for the larger test pulse, the depletion correction had a more pronounced effect on the release records for the larger test pulses (Fig. 8 *B*) than for the smaller test pulses (Fig. 8 *A*). Consequently, although *P/S* was quite similar for the test pulses to −20 and +20 mV without prepulses in the release records before correction for depletion, the depletion-corrected release records exhibited a smaller *P/S* for the larger test pulse than for the smaller one.

Fig. 9 *A* presents the $[Ca^{2+}]$ dependence of the values of peak rate of release (*P*) obtained from the depletion-corrected records in Fig. 8 and from several other

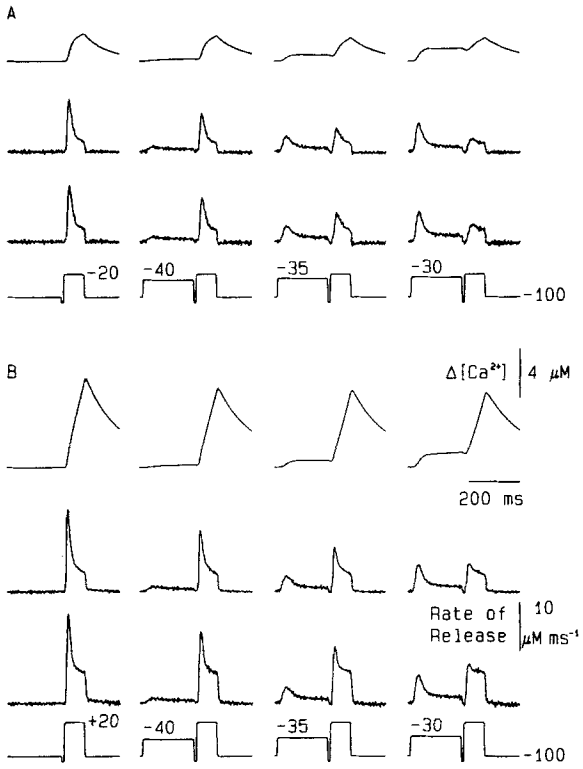

FIGURE 8. The effect of test pulse amplitude on inactivation of the peak R_{rel}. (*A*) *Top row*, $\Delta[Ca^{2+}]$ for a test pulse to −20 mV alone (*left*) or preceded by a 200-ms prepulse to −40, −35, or −30 mV. *Second row*, R_{rel} calculated from the corresponding Ca^{2+} records above. *Third row*, R_{rel} corrected for depletion of Ca^{2+} from the SR. The pulse protocol is shown at the bottom. (*B*) Same format and pulse protocol as *A*, but with a test pulse to +20 mV. The Ca^{2+} removal model parameters used for calculating R_{rel} were $k_{off,Mg\text{-}Parv}$ = 7.1 s^{-1}, pump V_{max} = 949 μM s^{-1}, and [Parv] = 408 μM. The initial SR Ca^{2+} content was assumed to be 1.2 mM. Fiber 479, [AP III] 768–843 μM, resting $[Ca^{2+}]$ 26–29 nM, sarcomere length 4.0 μm, temperature 8°C.

records (not shown) from the same fiber. *P* is plotted rather than *P/S* − 1 to emphasize the difference in the amplitude of peak release for the different test pulses. The pulse sequence was first applied with the test pulse to −20 mV (open circles), then with the test pulse to +20 mV (squares), and finally a single test pulse to −20 mV was applied (filled circle). The peak release for the final test pulse to −20 mV was essentially the same as for the test pulse alone in the initial sequence (open circles at lowest $[Ca^{2+}]$), indicating that run down was not significant over the the course of this experiment. The lines in Fig. 9 represent the values of *P* predicted from the best fit of Eq. 6 to the values of *P/S* − 1 for the runs with test pulses to −20 or +20 mV. The values of the parameters obtained from the fits, 0.38 μM and 1.84

for Ca_{50} and n using the test pulse to −20 mV and 0.42 μM and 1.72 using the test to +20 mV, were quite similar for the two different test pulses. The similarity of the calcium dependence of inactivation for the two test pulses is shown graphically in Fig. 9 *B*, which presents the percent inactivation $[(P/S - 1)K_S/f_P]$ predicted by the two sets of data and the two independent fits. There is no indication of any appreciable difference in the calcium dependence of the degree of inactivation obtained using the two different test pulses. Similar results were obtained in two other fibers using the protocol of Figs. 8 and 9. Thus, the determination of the degree of inactivation at the

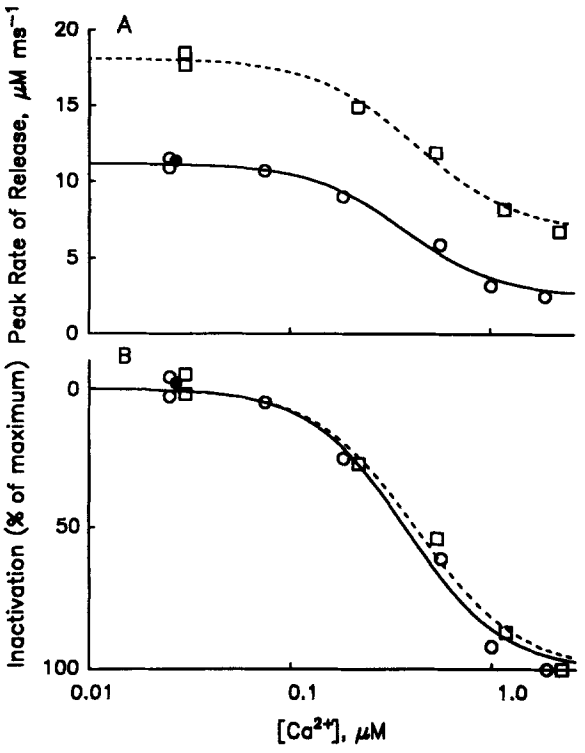

FIGURE 9. The $[Ca^{2+}]$ dependence of inactivation of the peak R_{rel} for different amplitude test pulses. (*A*) The peak R_{rel} during the test pulse versus $[Ca^{2+}]$ at the end of a 200-ms prepulse. *Circles*, Values of peak R_{rel} during a test pulse to −20 mV; *squares*, peak R_{rel} during a test pulse to +20 mV. The filled circle represents a value with a test pulse to −20 mV, recorded after the sequence of six records with a test pulse to +20 mV. (*B*) Same data as in *A*, normalized to represent the inactivatable release, expressed as a percentage of the maximal inactivation. The theoretical lines in *A* and *B* are least-squares fits of Eq. 6 to the data with Ca_{50} = 0.38, f_P/K_S = 3.55, n = 1.84 (*solid*); and Ca_{50} = 0.42 μM, f_P/K_S = 1.63, and n = 1.72 (*dashed*). From the experiment shown in Fig. 8.

end of the prepulse does not appear to be influenced by the degree of activation in the test pulse used to determine inactivation, consistent with a calcium-dependent inactivation process that operates independently of the activation mechanism.

Inactivation of Release Occurred without Suppression of Charge Movement

In several fibers intramembrane charge movement was measured during the pulses used to determine inactivation of calcium release. Fig. 10 gives results from one such fiber. The top row of Fig. 10 presents calcium transients for a 100-ms test pulse to −20 mV (left column), for the same test pulse preceded by a 200-ms prepulse to −40 mV (middle column), and for the same prepulse by itself (right column). The pulse diagrams are shown at the bottom of each column. The test pulse was directly preceded by a 10-ms step to −120 mV as in all inactivation experiments. For the

experiments in this section the prepulse without test pulse was followed by a 110-ms step to −120 mV to permit determination of the OFF charge movement during the first 10 ms of the step to −120 mV after the prepulse (see Methods). The second row of Fig. 10 shows records of the rate of calcium release calculated from each of the $\Delta[Ca^{2+}]$ records in the top row. In this fiber the release for the test pulse alone (second row, left) exhibited a very pronounced decline from its early peak. The release record for the test pulse after the prepulse (second row, middle) shows that

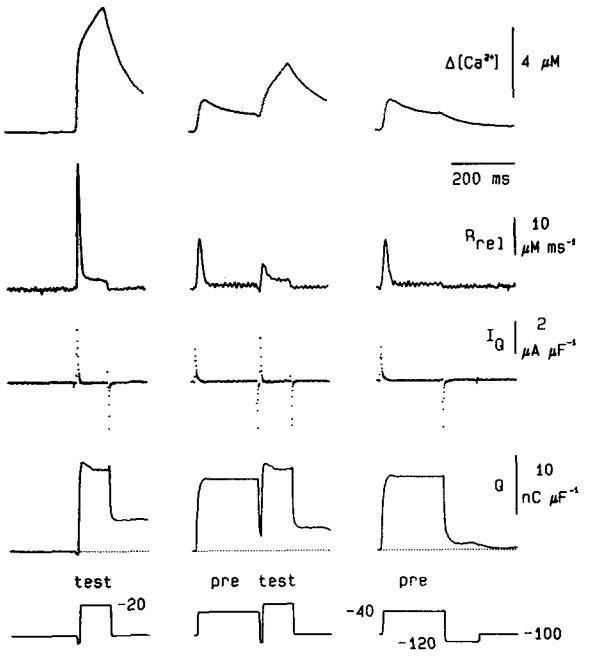

FIGURE 10. Intramembrane charge movement currents recorded for the inactivation protocol. *Top row,* $\Delta[Ca^{2+}]$ for (from left to right) a test pulse depolarization of 100 ms to −20 mV, the same test depolarization preceded by a 200-ms prepulse to −40 mV, and the 200-ms prepulse followed by a 110-ms hyperpolarization to −120 mV. *Second row,* The R_{rel} calculated from the corresponding $\Delta[Ca^{2+}]$ records above. *Third row,* Intramembrane charge movement currents (I_Q) recorded simultaneously with the $\Delta[Ca^{2+}]$ records. *Fourth row,* The charge (Q) moved during the records, obtained as the running integral of the corresponding current records. The pulse protocol is shown at the bottom, with pre- and test pulses as indicated. Before calculating Q the value of I_Q during the final 100 ms of both prepulses was set to zero. Since the 10-ms interval was too brief to establish a final baseline, the current during the 10-ms hyperpolarization of the middle record was taken from the first 10 ms after the prepulse of the right-most I_Q record and the current during the 10-ms hyperpolarization preceding the test pulse alone (left record) was taken from the first 10 ms of the I_Q record (not shown) for a 100-ms, 20-mV hyperpolarization from the holding potential. For the calculation of R_{rel}, Ca^{2+} removal model parameters were $k_{off,Mg\text{-}Parv}$ = 4.3 s^{-1}, pump V_{max} = 1,167 μM s^{-1}, and [Parv] was set to 600 μM. Fiber 453, [AP III] 580–776 μM, resting $[Ca^{2+}]$ assumed to be 50 nM, sarcomere length 4.1 μm, temperature 9°C.

the inactivatable component of release during the test pulse (second peak in the record) was largely suppressed when the test pulse was preceded by the prepulse. Comparison of P/S − 1 for the release records for the test pulses with and without prepulses in Fig. 10 indicates that inactivation of release was at least 84% of the maximal level at the end of the prepulse.

The third row of Fig. 10 presents the charge movement currents (I_Q) calculated from the total currents recorded simultaneously with each of the calcium transients.

For the test pulse alone (left) or the prepulse alone (right) the I_Q records exhibit an outward transient during the pulse and an inward transient after the pulse. The two negative points preceding the test pulse (left) occurred during the 10-ms hyperpolarization before the test pulse and were due to a slightly larger transient during the ON than during the OFF of a 20-mV hyperpolarization from −100 mV. This was observed systematically in all fibers and probably was due to a relatively small, nonlinear, time-dependent ionic current during the 20-mV hyperpolarization. The likely presence of this ionic current during the ON was the reason for using only the OFF of the 20-mV hyperpolarization for the control transient (Methods). The single positive point at the OFF of the test pulse alone (left) was not a systematic finding in the records from the other fibers. For the test pulse after the prepulse (middle) there is an outward I_Q during the prepulse, an inward I_Q during the 10-ms step to −120 mV, a second outward I_Q during the test pulse, and finally, a second inward I_Q after the test pulse. The I_Q component during the test pulses was somewhat smaller when the test pulse was preceded by a prepulse (middle) than when the test pulse was applied alone (left). This was due to the fact that the 10-ms step to −120 mV between the pre- and test pulses was not sufficiently long to allow return of all charge that had moved during the prepulse.

The fact that the prepulse charge was not fully returned by the end of the 10-ms gap is shown more clearly by examining records of total charge moved (Q), obtained as the running integral of I_Q and presented in the next to bottom row of records in Fig. 10. When the test pulse was preceded by a prepulse (middle), Q did not quite return to baseline by the end of the 10-ms gap between pre- and test pulses. However, the Q records indicate that during the test pulses Q attained essentially the same level and followed a very similar time course whether the test pulse was applied alone (left) or was preceded by the prepulse (middle). Indeed, for this fiber the cumulative Q values were identical at the end of the test pulses without and with the prepulse, 14.1 nC μF^{-1}.

Table II presents values of cumulative charge movement from four fibers studied using pulse protocols similar to those in Fig. 10. The left side of Table II lists the cumulative ON charge at the end of test pulses without and with prepulses. In all cases the cumulative test pulse Q_{ON} was very similar without and with the prepulse. The mean values of the cumulative charge at the end of the test pulse were 15.5 ± 1.3 nC μF^{-1} with a prepulse, and 15.6 ± 1.3 nC μF^{-1} without a prepulse (Table II). These values are not significantly different ($P > 0.9$, two-tailed t test). The mean (±SEM) difference in cumulative test pulse Q_{ON} values (without minus with the prepulse) was 0.1 ± 1.1 nC μF^{-1}, which is not significantly different from zero (Table II, $P > 0.9$). Thus, prepulses that produced marked inactivation of test pulse calcium release produced no significant suppression of charge movement during the test pulse. Since the charge movement during the test pulse was hardly altered by the prepulse, the pronounced inactivation of test pulse calcium release produced by the prepulse cannot be attributed to an effect of the prepulse on the charge movement during the test pulse.

Three additional observations were made concerning the charge movements measured using this pulse protocol. First, during the test pulses both with and without prepulses in Fig. 10 the initial outward I_Q was followed by a period during

which I_Q was slightly negative. Although this negative phase is barely noticeable in the I_Q records in Fig. 10 (row 3, left and middle), it did cause a significant decline in test pulse Q during the pulse (row 4, left and middle). However, the decline in Q during the test pulse was essentially the same with or without the prepulse. This negative I_Q may have been due to a time-dependent ionic current during the test pulse that was not correctly removed with the straight, sloping baseline.

Second, during the prepulses in Fig. 10 and in all other fibers I_Q was systematically greater than zero during the second half of the 200-ms prepulse, although this is hardly detectable in the I_Q records in Fig. 10 (row 3, middle and right). If the prepulse I_Q had been integrated over this interval, a delayed additional positive Q of a few nanocoulombs per microfarad would have been prominent in the Q record during the second half of the prepulses. However, since the positive I_Q during the second half of the prepulse could reflect a slight error in baseline subtraction, we stopped the integration of I_Q during the second half of each prepulse in calculating

TABLE II

Cumulative Charge Movement by the End of the ON and OFF Intervals of Test Pulses with and without Prepulses

Fiber reference	Prepulse	Cumulative test Q_{ON}			Cumulative test Q_{OFF}		
		Without prepulse	With prepulse	Without − with	Without prepulse	With prepulse	Without − with
	mV		*nC μF⁻¹*			*nC μF⁻¹*	
451	−40	19.0	20.1	−1.1	6.8	5.4	1.4
453	−40	14.1	14.1	0.0	5.3	3.9	1.4
454	−35	16.3	15.1	1.2	3.3	1.8	1.5
454	−35*	16.5	13.5*	3.0	3.9	0.3*	3.6
492	−45*	12.0	14.8*	−2.8	1.4	2.5*	−1.1
Mean ± SEM		15.6 ± 1.3	15.5 ± 1.3	0.1 ± 1.1	4.1 ± 1.0	2.8 ± 1.0	1.4 ± 0.8

*For these sequences a given test pulse was applied alone and after each of three different prepulses, one to the indicated voltage and one each to the indicated voltage ±5 mV. The starred values give the average for the test pulse after the three prepulses.

the Q records in the middle and left of Fig. 10 and for all other prepulse charge movement calculations. Thus the Q records are flat and noise free during the second half of each prepulse in Fig. 10. The downward droop in Q after the prepulse alone in Fig. 10 (row 4, right) also presumably represents a systematic baseline error rather than an additional movement of charge due to the step from −120 to −100 mV, since here and in other fibers the droop began before the step, which without the prepulse was the step used for defining the fiber linear capacitance.

Third, the cumulative Q records in Fig. 10 (fourth row of records) show that after the test pulses the measured cumulative Q did not return to zero either without (left) or with (middle) the prepulse, indicating an imbalance in the charge moved outward during depolarization and the charge moved inward during repolarization. Possible explanations for the observed charge imbalance will be considered in the Discussion. An interesting aspect of the charge imbalance after the test pulses in Fig. 10 was that the imbalance was smaller when the test pulse was preceded by the prepulse. Since

the cumulative Q_{ON} at the end of the test pulse was the same with and without the prepulse (above), the prepulse had the effect of increasing the amount of inward charge movement in the I_Q transient after the test pulse.

The preceding observations concerning charge imbalance were characteristic of all fibers studied. The right side of Table II lists the values of cumulative Q_{OFF} after the test pulses in pulse protocols similar to those at the bottom of Fig. 10. The values of cumulative test pulse Q_{OFF} were systematically greater than zero, corresponding to a charge imbalance after the test pulses as shown in the Q records in Fig. 10. The mean value of cumulative Q_{OFF} was 4.1 ± 1.0 nC μF^{-1} for test pulses without prepulses and 2.8 ± 1.0 nC μF^{-1} for test pulses after prepulses, both of which are significantly different from zero ($P < 0.05$ in both cases). As in Fig. 10, the charge imbalance after the test pulses was generally less when the test pulse was preceded by a prepulse. However, the mean difference in cumulative test pulse Q_{OFF} values (without minus with prepulse) of 1.4 ± 0.8 nc μF^{-1} is not significantly different from zero ($P < 0.1$). For the sequences in Table II there was a mean increase of 1.4 ± 0.4 nC μF^{-1} in the individual OFF charge movement for test pulses after prepulses compared with test pulses applied without prepulses (data not presented in Table II), which is significantly different from zero. In the same sequences, the mean cumulative Q_{OFF} after the prepulses without test pulse was 0.3 ± 0.4 nC μF^{-1} (data not presented in Table II). This value is negligible compared with the mean Q_{ON} of 13.0 ± 1.6 nC μF^{-1} for the prepulses in these sequences (data not presented in the table) and is not significantly different from zero ($P > 0.4$). Thus, there was negligible charge imbalance after the prepulses themselves, whereas there was a significant charge imbalance after the test pulses using the present pulse protocol. Although these observations concerning charge balance are interesting with regard to the properties of charge movement and will be considered in this regard in the Discussion, it is important to note that they do not alter the conclusion that prepulses which produced near maximal inactivation of release during the subsequent test pulse produced no suppression of charge movement during the test pulse.

Alternative Assumptions Concerning Intrinsic Calcium Buffers

Our calculation of the rate of calcium release does not require any assumptions concerning the calcium-binding and transport systems that remove calcium relatively slowly from the myoplasm. The properties of these systems are characterized in each fiber by adjusting the removal system model parameters so as to reproduce the decline of $\Delta[Ca^{2+}]$ in that fiber. In contrast, our release calculation does require assumptions concerning the rapidly equilibrating calcium-binding sites intrinsic to the fiber (Melzer et al., 1987). It is therefore important to examine the extent to which present conclusions concerning the calcium dependence of inactivation might be influenced by assumptions regarding the rapidly equilibrating intrinsic calcium-binding sites.

Fig. 11 illustrates release calculations made using three different sets of assumptions concerning the intrinsic fast calcium-binding sites. For the left column, labeled "200 μM [Pump]," the fast intrinsic sites were assumed to consist of 250 μM troponin C and 200 μM SR calcium pump sites, the standard assumptions used thus far in this paper. For the middle column, labeled "1 μM [Pump]," the concentration of

troponin C was again 250 μM, but the concentration of pump sites was reduced to 1 μM, virtually eliminating the contribution of the pump sites to the total pool of fast calcium-binding sites. For the right column, labeled "linear fast buffer," the fast calcium-binding sites of both troponin C and the pump were replaced by a single hypothetical instantaneous calcium-binding site that always bound an amount of calcium corresponding to 20 times $[Ca^{2+}]$. Each of the panels in the top row of Fig. 11

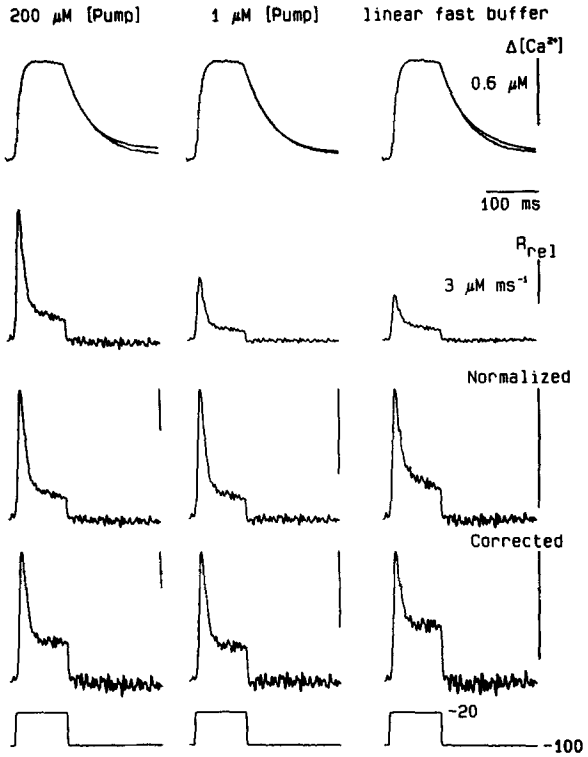

FIGURE 11. Calcium release records based on different assumptions for the rapid myoplasmic Ca^{2+} buffers. *Top row,* The measured $\Delta[Ca^{2+}]$ for a 100-ms depolarization to −20 mV is shown in each column. Superimposed on the measured $\Delta[Ca^{2+}]$ record is the predicted decay of $\Delta[Ca^{2+}]$ calculated from one of three models of the intrinsic rapid Ca^{2+} buffers, beginning 14 ms after the end of the depolarization (see text for a description of the different assumptions). *Second row,* R_{rel} calculated from the $\Delta[Ca^{2+}]$ record shown, using one of the three assumed models as indicated. *Third row,* R_{rel} normalized to the maximum value of the peak. *Fourth row,* R_{rel} corrected for SR Ca^{2+} depletion, then normalized to the maximum value of the peak. The relative timing of the depolarization is shown at the bottom. The following parameters were varied to characterize the Ca^{2+} removal properties of the fiber and to calculate the R_{rel} (see Melzer et al., 1987). 200-μM [Pump]: $k_{off,Mg\text{-}Parv} = 6.9\ s^{-1}$, pump $V_{max} = 1967\ \mu M\ s^{-1}$, [Parv] = 549 μM, initial SR Ca^{2+} content = 0.9 mM. 1-μM [Pump]: $k_{off,Mg\text{-}Parv} = 7.2\ s^{-1}$, pump $V_{max} = 609\ \mu M\ s^{-1}$, [Parv] set to 200 μM, initial SR Ca^{2+} content = 0.5 mM. Linear fast buffer: $k_{on} = 5.9\ \mu M^{-1}\ s^{-1}$, $k_{ns} = 228\ s^{-1}$, [total site] = 81 μM, initial SR Ca^{2+} content = 0.3 mM. Fiber 503, [AP III] 677–850 μM, resting $[Ca^{2+}]$ 12–19 nM, sarcomere length 4.0 μm, temperature 8°C.

presents the identical calcium transient (noisier traces) for a 100-ms test pulse to −20 mV without any prepulse (bottom of each column). The smooth lines close to the falling phase of each $\Delta[Ca^{2+}]$ record give the theoretical $\Delta[Ca^{2+}]$ predicted using the fit of the removal model to $\Delta[Ca^{2+}]$ starting 14 ms after the end of this and several other pulses of various amplitudes and durations. The relatively good agreement of

the two lines in each panel indicates that the removal model could reproduce the fall of $\Delta[Ca^{2+}]$ using each of the assumed properties for the fast intrinsic sites.

The second row of Fig. 11 presents the rate of release calculated from the $\Delta[Ca^{2+}]$ record in the top row using each of the assumptions concerning the fast sites. All three sets of assumptions give R_{rel} records that exhibit an early peak followed by a decline toward a maintained level (Melzer et al., 1987). However, the amplitude of the R_{rel} records decreases from left to right because of the decrease in the

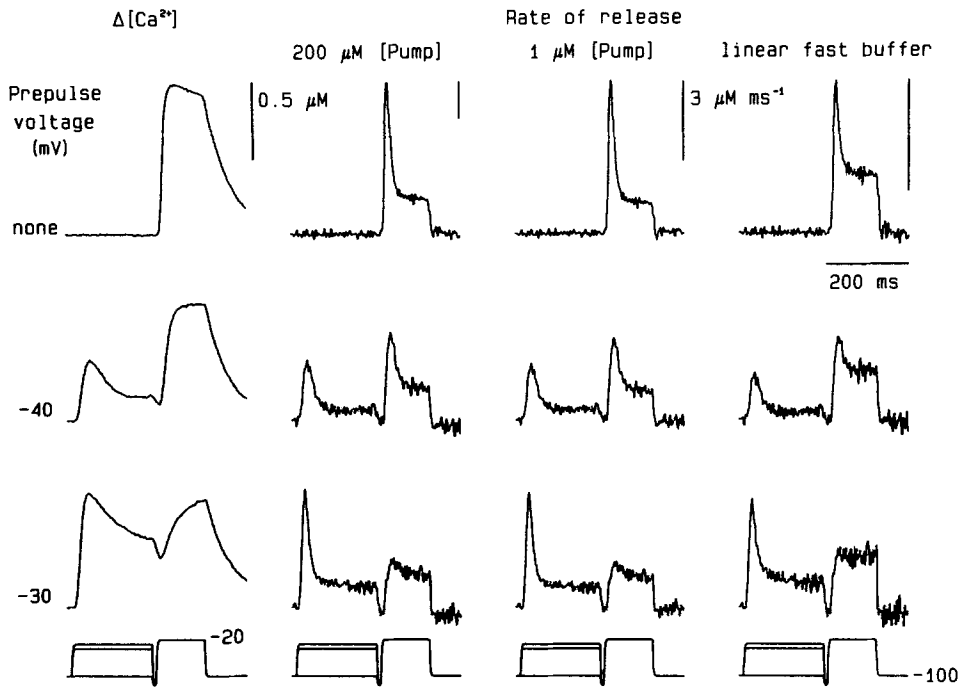

FIGURE 12. Effect of various assumptions for myoplasmic rapid Ca^{2+} buffers on the calculated inactivation of peak R_{rel} by a prepulse. Left column, $\Delta[Ca^{2+}]$ for a 120-ms test pulse to −20 mV, alone (*top*) or preceded by a 200-ms prepulse to −40 mV (*second row*) or −30 mV (*third row*). Right-most three columns, rate of Ca^{2+} release calculated from the corresponding $\Delta[Ca^{2+}]$ record to the left, using one of three assumed models for the rapid Ca^{2+} buffers as indicated. The pulse protocol is shown at the bottom. Same fiber, conditions, and removal model parameters as described in Fig. 11 legend.

concentration assumed for the fast calcium-binding sites. The third row of Fig. 11 presents the release records from the second row scaled to have the same peak amplitude. Comparison of the normalized records shows that they all have fairly similar time courses even though they were calculated using different assumptions concerning the fast intrinsic sites. The fourth row of records in Fig. 11 presents the release records corrected for depletion of calcium from the SR, again scaled to the same peak amplitude. The ratio of peak to steady release in the depletion-corrected

records is smaller assuming linear fast binding sites (right column) than for the other two sets of assumptions that use saturable sites. This is because the linear fast sites maintain a constant ratio of bound to free calcium during peak and steady release, whereas for the other models the ratio of bound to free calcium decreases at the higher $[Ca^{2+}]$ that is present during the steady phase of release.

Fig. 12 presents records from the same fiber as in Fig. 11 for the test pulse alone (top row) and for the test pulse preceded by a 200-ms prepulse to −40 mV (second row) or −30 mV (third row). The left column in Fig. 12 presents the calcium transient for a given pre- and test pulse combination, and the next three columns present

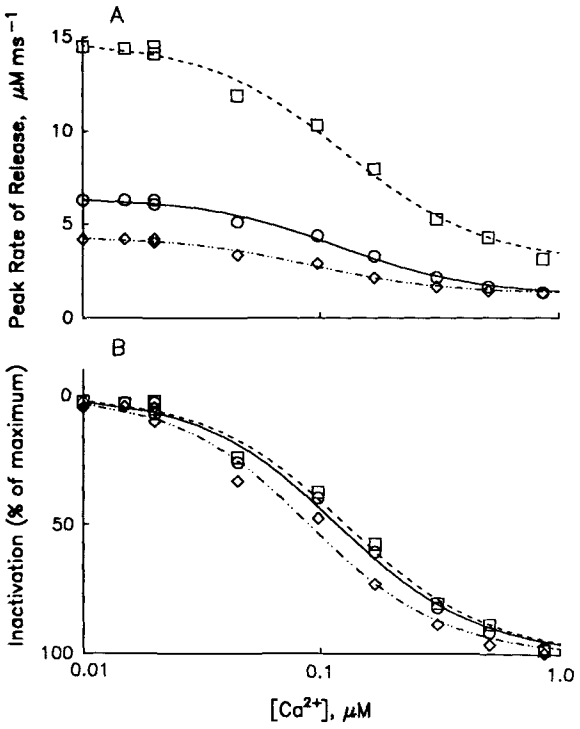

FIGURE 13. The dependence of peak rate of release on $[Ca^{2+}]$ for various assumptions for rapid myoplasmic Ca^{2+} buffers. (*A*) Peak rate of release versus the $[Ca^{2+}]$ measured at the end of a 200-ms prepulse. The data are from the experiment of Fig. 12 and several other records not shown. (*B*) The inactivatable component of release for each set of assumptions is normalized and expressed as the percentage of maximal inactivation. *Squares*, data assuming the rapid myoplasmic Ca^{2+} buffers to consist of 200-μM [Pump] sites; *circles*, 1-μM [Pump] sites; *diamonds*, linear fast buffer. The theoretical lines are least-squares fits of Eq. 6 to the data, with Ca_{50} = 0.13 μM, f_P/K_S = 4.00, n = 1.48 (*dashed line*); Ca_{50} = 0.12 μM, f_P/K_S = 4.26, n = 1.48 (*solid line*); and Ca_{50} = 0.09, f_P/K_S = 2.33, n = 1.54 (*dot-dashed line*).

three alternative release records calculated from $\Delta[Ca^{2+}]$ for the three alternative sets of assumptions concerning the fast intrinsic sites used in Fig. 11. The release records in each column of Fig. 12 have been corrected for depletion of calcium from the SR and scaled to give the same peak amplitude for the test pulse without prepulse. For each set of assumptions concerning the fast intrinsic sites, increasing the prepulse increasingly suppressed the peak release in the subsequent test pulse.

Fig. 13 *A* presents values of the peak rate of release during the test pulses of Fig. 12 and during six other test pulses applied with or without prepulses (records not shown). Each symbol represents a different set of assumptions concerning the fast

intrinsic sites. The three lines in Fig. 9 represent the values of P predicted from the best fit of Eq. 6 to the values of $P/S - 1$ for each of the three sets of calculated values. The values of n and Ca_{50} obtained from the three fits (Fig. 13 legend) were quite similar for the three alternative assumptions concerning the fast intrinsic sites. The similarity of the inactivation analyses for the three sets of release calculations is shown graphically in Fig. 13 *B*, where each set of data and its fit are presented in terms of percent inactivation as calculated from the fit parameters in Fig. 13 *A*. The points and fit for 250 μM troponin C with either 200-μM pump sites (squares and dashed line) or 1-μM pump sites (circles and solid line) are very close to each other. The data and fit for the linear intrinsic fast sites (diamonds and dot-dashed line) are just slightly to the left of the results using the other assumptions. Calcium transients from each of the 10 fibers in Table I were analyzed using the three sets of assumptions in Figs. 10–12. The resulting mean ± SEM values of Ca_{50} and n were 0.34 ± 0.05 and 1.87 ± 0.22 for 250 μM troponin C with 200-μM pump sites (Table I), 0.29 ± 0.05 and 1.70 ± 0.13 for 250-μM troponin C with 1-μM pump sites, and 0.31 ± 0.05 and 1.97 ± 0.11 for the linear, fast, intrinsic sites. None of these values are significantly different among the three data sets. Thus, the assumptions concerning the intrinsic, fast, calcium-binding sites had essentially no effect on the calculated calcium dependence of inactivation of release.

DISCUSSION

Determination of the Calcium Dependence of Inactivation

A major objective of this paper was the development and testing of a procedure for determining the equilibrium calcium dependence of the inactivation of calcium release from the SR in skeletal muscle fibers. The standard procedure used 200-ms prepulses of various amplitudes to elevate $[Ca^{2+}]$ to various steady levels. The peak rate of calcium release during a constant test pulse after each prepulse was used to monitor the degree of inactivation that had developed by the end of the prepulse. A 10-ms hyperpolarization was interposed between the pre- and test pulses in order to reset the TT voltage sensor before each test pulse. Since $[Ca^{2+}]$ declined only slightly during this 10-ms gap, and since previous results showed that recovery from inactivation is relatively slow (Schneider and Simon, 1988), little if any recovery from inactivation should have occurred during the gap between the pre- and test pulses. Tests of the procedure showed that the same calcium dependence was obtained using either different duration prepulses or different amplitude test pulses. A crucial aspect of the procedure was the use of calculated calcium release records to determine the suppression of release after a prepulse. The alternative procedure of using the amplitude of the $[Ca^{2+}]$ transient for a given test pulse to determine suppression of release after a prepulse would be unlikely to provide accurate estimates because of the elevation of $[Ca^{2+}]$ due to the prepulse and the complex relationship between the rate and time course of calcium release and the resulting $[Ca^{2+}]$ transient.

The calcium dependence of suppression of peak test release indicated that binding of more than one calcium ion was required to inactivate each channel and that half of the maximal degree of inactivation was attained at a free calcium concentration of ~0.3 μM (Table I). The magnitude of this $[Ca^{2+}]$ value is based on two important

assumptions. First, it was assumed that all of the AP III in the fiber was available to react with calcium. If the AP III that may be bound in the fiber were in a form unreactive with calcium, the actual calcium concentration could have been up to seven to nine times higher (Baylor et al., 1986; Maylie et al., 1987; Hirota et al., 1989). Second, since our calcium measurements are spatial average values, our estimate of the $[Ca^{2+}]$ for half-inactivation implicitly assumes that the true $[Ca^{2+}]$ at the inactivation site is equal to the spatial average. If the inactivation sites are located close to the release site, as seems likely, the local calcium concentration at the inactivation sites could actually have been considerably higher than the measured spatial average. Recent experiments using calcium release from "caged" calcium indicate that the actual $[Ca^{2+}]$ for inactivation may in fact be considerably higher than the measured global average $[Ca^{2+}]$ (Hill and Simon, 1991). Our measurement of the $[Ca^{2+}]$ for half-maximal inactivation may thus represent a lower limit on the actual value.

Calcium-dependent Inactivation of Release in Other Muscle Preparations

Inhibition of calcium release by elevated $[Ca^{2+}]$ has also been observed with other more disrupted preparations in which release was activated by elevated $[Ca^{2+}]$ rather than by TT depolarization. Using a rapid filtration technique to dilute heavy SR vesicles isolated from rabbit skeletal muscle into various release media, the rate of $^{45}Ca^{2+}$ efflux from passively loaded vesicles was found to be activated at submicromolar and micromolar $[Ca^{2+}]$ but inhibited at higher $[Ca^{2+}]$ (Meissner et al., 1986). Hill analysis indicated the inhibition to exhibit positive cooperativity (Meissner et al., 1986) as in the present experiments. However, half-maximal inhibition occurred at 150 μM $[Ca^{2+}]$ (Meissner et al., 1986), almost three orders of magnitude higher than found in the present experiments. Although the present value may underestimate the true $[Ca^{2+}]$ for inactivation (above), the underestimate is unlikely to be so large. In another study using native rabbit heavy SR vesicles incorporated into planar lipid bilayers, the open probability of single SR release channels continued to increase as $[Ca^{2+}]$ was increased to 950 μM and only began to decrease at higher $[Ca^{2+}]$ (Smith, Coronado and Meissner, 1986), indicating an even larger discrepancy with the present results. Furthermore, Ca^{2+} and Mg^{2+} were equally effective in producing the inactivation of calcium efflux observed by Meissner et al. (1986) and in blocking potassium currents through purified ryanodine receptors incorporated into planar lipid bilayers (Smith, Imagawa, Ma, Fill, Campbell, and Coronado, 1988). In the present experiments the internal solution contained ~1 mM free $[Mg^{2+}]$ so that relatively modest elevations of $[Ca^{2+}]$ could not have produced the observed marked inactivation of release via a mechanism that was equally sensitive to Ca^{2+} and Mg^{2+}.

The preceding considerations indicate that the inhibition studied in the present work could reflect a different process than that seen at higher $[Ca^{2+}]$ in the vesicle (Meissner et al., 1986) or bilayer (Smith et al., 1986, 1988) studies. If the inactivation process that we have studied was present in SR calcium channels incorporated into bilayers, it would not have been revealed by measurements of the equilibrium calcium dependence of channel open probability if it operated via a higher affinity calcium-binding site than the calcium-dependent activation process that opened the channels in the bilayer. In that case the equilibrium calcium dependence of channel open

probability determined in the bilayer experiments would simply reflect the calcium dependence of the activation process at an almost constant, near-maximal (but not complete) level of inactivation from the process studied here. In the vesicle studies of Meissner et al. (1986) the calcium loading was carried out at a relatively high [Ca^{2+}], one that would have produced maximal inactivation by the process studied in the present experiments. To initiate calcium release, the calcium-loaded vesicles were diluted into solutions of sufficiently elevated [Ca^{2+}] to produce release activation. If the inactivation process had a higher affinity than the activation process, inactivation would not have been reversed so that the calcium dependence of activation would again have been studied at a constant maximal level of inactivation. Despite these possibilities, it is still not certain whether the inhibition observed here and that observed with the more disrupted preparations actually represents a different inactivation process. It is still conceivable that the inactivation process could have exhibited different properties depending on whether the release system were still coupled to, and activated by, the TT voltage sensor as in the present experiments, or uncoupled from the TT sensor as in the more disrupted preparations.

In mechanically skinned frog skeletal muscle fibers, calcium release due to caffeine has been shown to be suppressed by elevated [Ca^{2+}] (Kwok and Best, 1987). The suppression of release in the experiments of Kwok and Best (1987) occurred over a similar range of [Ca^{2+}] as that found to produce inactivation of release in the present experiments. The calcium release produced by depolarization of voltage-clamped frog fibers is potentiated by caffeine and both the potentiated release and the control release in the absence of caffeine appear to undergo the same inactivation process (Klein et al., 1990), indicating that the inactivation studied by Kwok and Best (1987) and in this work are likely to reflect the same process. In mechanically skinned cardiac cells elevated [Ca^{2+}] has been shown to produce an inactivation of calcium-induced calcium release (Fabiato, 1985). This inactivation occurred with a delay and had an affinity for Ca^{2+} in the submicromolar range (Fabiato, 1985), as observed for the calcium-dependent inactivation of release studied in the present experiments.

Calcium Binding Models for Inactivation

The observed calcium dependence of the suppression of peak release was analyzed in Results using a specific calcium-binding model for the development of inactivation (Scheme 1). The model assumed rapidly equilibrating binding of n calcium ions to a receptor (R) on the calcium channel to give the complex Ca_nR, with the binding exhibiting infinite positive cooperativity. The binding step was assumed to be followed by a slower conformational change of Ca_nR to the inactivated state (Ca_nR^*) of the channel. Analysis of the calcium dependence of inactivation with this model showed unambiguously that the value of n was > 1. In 10 fibers, the mean value of n found with the infinitely cooperative model was 1.87 ± 0.22. This is a minimum estimate for the number of calcium ions that would have to bind in order to produce inactivation. If the binding actually were less highly cooperative, the true value for n would be higher.

A calcium-binding model for inactivation which differs slightly from Scheme 1 has been presented previously for $n = 1$ and has been shown to be formally identical to Scheme 1 with $n = 1$ under appropriate conditions (Schneider and Simon, 1988).

This model can also be generalized to include the binding of n calcium ions. In this model the free receptor R binds calcium but is not part of the calcium channel. The Ca_nR complex then produces inactivation by binding to the channel rather than by undergoing a conformational change as in Scheme 1. Since this model is formally identical to Scheme 1, it would give the same n values as obtained with the model in Scheme 1.

The calcium-binding model for inactivation in Scheme 1 and the model described in the preceding paragraph are both based on the assumption that the SR calcium release channels constitute a single uniform population. The observation that inactivation was not complete, even at saturating $[Ca^{2+}]$, was accounted for in these models by including a calcium-independent transition after the calcium-binding steps. The maximal extent of inactivation depended on the equilibrium of the calcium-independent step. Previous work indicated that a calcium-independent step was necessary to account for the observation that for intermediate and large depolarizations the rate of development of inactivation did not increase with increasing $[Ca^{2+}]$ (Melzer et al., 1984; Schneider and Simon, 1988).

There is an alternative interpretation for the finding that inactivation of calcium release was never complete. If there were actually two populations of SR calcium release channels, one completely inactivating and one noninactivating, the overall calcium release would appear to inactivate incompletely. In this case, the steady release would be due to release through noninactivating channels. The ratio of peak to steady release would depend both on the maximum available release through each type of channel and on the values of the activation and inactivation factors for each type of channel at the time of peak release.

Previous results indicate that if there are two types of channel they exhibit very similar time courses of activation (Simon and Schneider, 1988). Assuming the activation time course to be the same for the activating and noninactivating channels, the release through the inactivating channels at the time of peak release would be given by

$$P - Sa_P/a_s = A_I a_P b_P \tag{10}$$

where A_I is the maximum release through the inactivating channels. Since S is equal to $a_S A_N$, where A_N is the maximum release through the noninactivating channels, Eq. 10 can be expressed as

$$a_S P/a_P S - 1 = b_P A_I/A_N \tag{11}$$

Defining a correction factor h_P as b_P/b_{pre},

$$a_S P/a_P S - 1 = b_{pre}\, h_P A_I/A_N \tag{12}$$

If h_P were the same for test pulses after all prepulses, $a_S P/a_P S - 1$ would be proportional to the fraction of the inactivatable channels that were not inactivated at the end of the prepulse.

If there were two types of channels, the calcium-binding model in Scheme 1 might not be appropriate to account for inactivation of the completely inactivating channels. With this model, when $[Ca^{2+}]$ is sufficiently elevated to produce complete

inactivation, the forward rate constant for the development of inactivation would have to greatly exceed the reverse rate constant in order for the channels to inactivate completely. In this case the rate constant observed for development of inactivation would equal the forward rate constant for the slow Ca_nR to Ca_nR^* transition. In contrast, during recovery from inactivation at low $[Ca^{2+}]$ the opposite would have to be true to account for complete recovery, and the rate constant observed for recovery would equal the reverse rate constant for the slow transition. Thus, for Scheme 1 to be a viable model for a completely inactivating channel, the rate of recovery from inactivation would have to be much slower than the rate of development of inactivation. However, the observed rate constant for recovery from inactivation after a pulse was only about three times slower than the rate of development of inactivation during the pulse (Schneider and Simon, 1988). We have previously pointed out that this observation poses a kinetic difficulty when using models such as Scheme 1 to represent a completely inactivating channel.

One way to circumvent the kinetic problem in using Scheme 1 to account for inactivation of a completely inactivating channel is to modify the model so that the fully calcium-occupied state Ca_nR no longer directly undergoes a transition to the inactivated state Ca_nR^*. Instead, Ca_nR could control the rate of another reaction, such as the phosphorylation or dephosphorylation of the channel. An example of control of inactivation by channel phosphorylation in another preparation may be the inactivation of surface membrane calcium channels in snail neurons by dephosphorylation and the reversal of that inactivation by phosphorylation (Chad and Eckert, 1986).

One model for control of inactivation by phosphorylation is

$$\mathrm{ATP} + \mathrm{C} \underset{\beta\{Ca_nR\}}{\overset{\alpha\{Ca_nR\}}{\rightleftharpoons}} \mathrm{ADP} + \mathrm{CP}^*$$

Scheme 2

where C is the unphosphorylated and noninactivated form of the channel, CP* is the phosphorylated and inactivated form of the channel, and $\alpha\{Ca_nR\}$ and $\beta\{Ca_nR\}$ are rate constants that are functions of Ca_nR. The functions α and β could increase and decrease, respectively, with Ca_nR; e.g., by Ca_nR activating the kinase and inhibiting the phosphatase responsible for the reactions. During elevated $[Ca^{2+}]$, $\alpha[Ca_nR]$ could greatly exceed $\beta[Ca_nR]$ and inactivation could develop completely due to full accumulation of CP*. When $[Ca^{2+}]$ declined the reverse would occur. In this case, however, both the development of and recovery from inactivation could exhibit similar time courses because both the forward and reverse rate constants for the reaction that determines inactivation could change reciprocally depending on the amount of Ca_nR.

For the model in Scheme 2, in the steady state

$$\alpha'\{Ca_nR\}\,C = \beta\,\{Ca_nR\}\,(1 - C) \tag{13}$$

where $\alpha'\,\{Ca_nR\}$ is the product of the ATP concentration and $\alpha\{Ca_nR\}$. Considering the case of infinitely cooperative binding of n calcium ions to the receptor R on the

left of Scheme 1,

$$Ca_nR = [Ca^{2+}]^n/(K_F + [Ca^{2+}]^n) \quad (14)$$

Arbitrarily assuming that the fractional activation of the kinase is equal to the fraction Ca_nR of receptor molecules with n calcium ions bound, and that the fractional inhibition of the phosphatase is equal to the fraction $1 - Ca_nR$ of receptors not occupied by calcium,

$$\alpha'\{Ca_nR\} = \alpha'_{max}Ca_nR \quad (15)$$

and

$$\beta\{Ca_nR\} = \beta_{max}(1 - Ca_nR) \quad (16)$$

Solving Eq. 13 for C, substituting Eqs. 14–16 in the resulting equation, and then substituting the result for b_{pre} in Eq. 12 gives

$$a_SP/a_PS - 1 = (h_PA_I/A_N)K'/(K' + [Ca^{2+}]^n) \quad (17)$$

where K' is $K_F\beta_{max}/\alpha'_{max}$. Eq. 17 is identical in form to Eq. 9 and will thus give the identical values of Ca_{50} and n as obtained by fitting Eq. 9 to the $a_SP/a_PS - 1$ data.

An alternative model that does not involve reciprocal activation and inhibition of the kinase and phosphatase is

$$\begin{array}{ccc} ATP + C & \underset{\beta}{\overset{\alpha\{Ca_nR\}}{\rightleftharpoons}} & ADP + CP \\ k_{off} \uparrow & & \downarrow k_{on}, \\ ATP + C^* & \underset{\beta}{\overset{\alpha\{Ca_nR\}}{\rightleftharpoons}} & ADP + CP^* \end{array}$$

Scheme 3

where C and CP are both noninactivated and C* and CP* are both inactivated. The function $\alpha\{Ca_nR\}$ would again increase with Ca_nR, but α is now independent of Ca_nR. In this model the phosphorylated form of the channel is much more likely to undergo inactivation than the unphosphorylated form. With appropriate selection of rate constants, development of inactivation could occur with rate constant k_{on} at elevated $[Ca^{2+}]$ and recovery from inactivation could occur with rate constants β and k_{off} when $[Ca^{2+}]$ returned to resting values. This model can also be shown to give a calcium dependence of inactivation having the same form as Eq. 17 and would thus also give the same values of n and Ca_{50} as obtained with Scheme 1.

Charge Movements with the Pulse Protocol for Inactivation

For purposes of understanding inactivation of calcium release, the principal present finding regarding charge movement was that inactivation occurred without significant suppression of charge movement during the test pulse used for monitoring the degree of inactivation of release. Thus, the calcium-dependent inactivation mechanism does not appear to operate via modification of the TT voltage sensor. The inactivation pulse protocol also revealed several other points regarding charge

movement. Although these points do not alter the conclusion that inactivation occurred without modification of charge movement during the test pulse, they may be of interest in regard to the charge movement process itself.

Our charge movement records indicated that the measured cumulative charge did not return to zero after the test pulses in our inactivation pulse protocol, either with or without prepulses. One possible explanation for such a charge imbalance might simply be improper selection of current baselines for calculating I_Q so that the outward I_Q during depolarization was overestimated or the inward I_Q during repolarization was underestimated, or both. In this regard it is important to note that the measured charge imbalance cannot be attributed to any inequality in the ON and OFF segments in the control current records used for removing linear capacitative current when calculating the charge movement current. In every case the ON and OFF segments of our control current records were both constructed from the identical average total current for the OFF of a 20-mV hyperpolarizing pulse.

An alternative explanation for the charge imbalance is that it might be due to a shift in the effective membrane voltage in the presence of elevated $[Ca^{2+}]$ so that the effective voltage at the end of the test pulse was significantly less negative than before applying the pulses (Csernoch, Uribe, Rodriquez, Pizarro, and Rios, 1989; Horowicz and Schneider, 1981). In this case a hyperpolarization would be required after the test pulse to reach the same effective voltage as before the pulse so as to restore charge to its resting distribution and thus produce a cumulative Q of zero. In this regard it is interesting that the prepulse without test pulse was followed by a 100-ms OFF step to −120 mV (Fig. 10, bottom right), rather than by a simple return to the −100-mV holding potential as was the case after the test pulses (Fig. 10, bottom left and middle). For the prepulse followed by the 100-ms hyperpolarization to −120 mV Q returned almost to zero after the pulse, even though the pulse did produce an appreciable elevation of $[Ca^{2+}]$ (top right). Unfortunately, the test pulses in these experiments were never followed by a similar hyperpolarization. Thus it is not known whether an after-hyperpolarization would have caused the return of further charge after the test pulses or whether such an after-hyperpolarization could have restored charge balance after the test pulses.

In conclusion, we found that prepulses that produce near-maximal inactivation of calcium release produce essentially no change in charge movement during the test release, indicating that the inactivation occurs at a step beyond the TT voltage sensor. The equilibrium calcium dependence of inactivation indicates that inactivation is produced by relatively modest increases of $[Ca^{2+}]$ above the resting level and that more than a single calcium ion must bind to produce the observed inactivation.

We thank Gerard Vaio for excellent technical assistance, Gabe Sinclair and Walt Knapik for custom modification of optical and mechanical apparatus, and Jeff Michael and Chuck Leffingwell for construction of electronic equipment.

This work was supported by research grants from the National Institutes of Health (NS-23346) and the Muscular Dystrophy Association. Dr. Klein was the recipient of an MDA postdoctoral fellowship.

Original version received 8 May 1990 and accepted version received 20 September 1990.

REFERENCES

Baylor, S. M., W. K. Chandler, and M. W. Marshall. 1983. Sarcoplasmic reticulum calcium release in frog skeletal muscle fibres estimated from Arsenazo III calcium transients. *Journal of Physiology.* 344:625–666.

Baylor, S. M., S. Hollingworth, C. S. Hui, and M. E. Quinta-Ferreira. 1986. Properties of the metallochromic dyes arsenazo III, antipyrylazo III and azo 1 in frog skeletal muscle fibres at rest. *Journal of Physiology.* 377:89–141.

Chad, J. E., and R. Eckert. 1986. An enzymatic mechanism for calcium current inactivation in dialysed *Helix* neurones. *Journal of Physiology.* 378:31–51.

Csernoch, L., I. Uribe, M. Rodriguez, G. Pizarro, and E. Rios. 1989. Q_γ and Ca release flux in skeletal muscle fibers. *Biophysical Journal.* 55:88*a*. (Abstr.)

Fabiato, A. 1985. Time and calcium dependence of activation and inactivation of calcium-induced release of calcium from the sarcoplasmic reticulum of a skinned canine cardiac Purkinje cell. *Journal of General Physiology.* 85:247–289.

Grynkiewicz, G., M. Poenie, and R. Y. Tsien. 1985. A new generation of Ca^{2+} indicators with greatly improved fluorescence properties. *Journal of Biological Chemistry.* 260:3440–3450.

Hill, D., and B. J. Simon. 1991. Use of "caged calcium" in skeletal muscle to study calcium-dependent inactivation of calcium release. *Biophysical Journal.* 59:239*a*. (Abstr.)

Hirota, A., W. K. Chandler, P. L. Southwick, and A. S. Waggoner. 1989. Calcium signals recorded from two new purpurate indicators inside frog cut twitch fibers. *Journal of General Physiology.* 94:597–631.

Horowicz, P., and M. F. Schneider. 1981. Membrane charge moved at contraction thresholds in skeletal muscle fibers. *Journal of Physiology.* 314:595–633.

Klein, M. G., B. J. Simon, and M. F. Schneider. 1990. Effects of caffeine on calcium release from the sarcoplasmic reticulum in frog skeletal muscle fibres. *Journal of Physiology.* 425:599–626.

Klein, M. G., B. J. Simon, G. Szucs, and M. F. Schneider. 1988. Simultaneous recording of calcium transients in skeletal muscle using high and low affinity calcium indicators. *Biophysical Journal.* 55:971–988.

Kovacs, L., E. Rios, and M. F. Schneider. 1983. Measurement and modification of free calcium transients in frog skeletal muscle fibres by a metallochromic indicator dye. *Journal of Physiology.* 343:161–196.

Kwok, W., and P. M. Best. 1987. Myofilament space calcium concentration affects the calcium release rate from the sarcoplasmic reticulum of skinned, skeletal muscle fibers of the frog. *Biophysical Journal.* 51:104*a*. (Abstr.)

Maylie, J., M. Irving, N. L. Sizto, and W. K. Chandler. 1987. Calcium signals recorded from cut frog twitch fibers containing antipyrylazo III. *Journal of General Physiology.* 89:83–143.

Meissner, G., E. Darling, and J. Eveleth. 1986. Kinetics of rapid Ca^{2+} release by sarcoplasmic reticulum: effects of Ca^{2+}, Mg^{2+}, and adenine nucleotides. *Biochemistry.* 25:236–244.

Melzer, W., E. Rios, and M. F. Schneider. 1984. Time course of calcium release and removal in skeletal muscle fibres. *Biophysical Journal.* 45:637–641.

Melzer, W., E. Rios, and M. F. Schneider. 1986*a*. The removal of myoplasmic free calcium following calcium release in frog skeletal muscle. *Journal of Physiology.* 372:261–292.

Melzer, W., E. Rios, and M. F. Schneider. 1987. A general procedure for determining calcium release from the sarcoplasmic reticulum in skeletal muscle fibers. *Biophysical Journal.* 51:849–863.

Melzer, W., M. F. Schneider, B. J. Simon, and G. Szucs. 1986*b*. Intramembrane charge movement and calcium release in frog skeletal muscle. *Journal of Physiology.* 373:481–511.

Schneider, M. F., and B. J. Simon. 1988. Inactivation of calcium release from the sarcoplasmic reticulum in frog skeletal muscle. *Journal of Physiology.* 405:727–745.

Schneider, M. F., B. J. Simon, and M. G. Klein. 1989. Decline of calcium release from the sarcoplasmic reticulum in skeletal muscle cells due to inactivation and calcium depletion. *In* Physiology and Pharmacology of Transmembrane Signaling. T. Segawa, M. Endo, M. Ui, and K. Kurihara, editors. Elsevier Science Publishers B.V., Amsterdam. 253–260.

Schneider, M. F., B. J. Simon, and G. Szucs. 1987. Depletion of calcium from the sarcoplasmic reticulum during calcium release in frog skeletal muscle. *Journal of Physiology.* 392:167–192.

Simon, B. J., M. G. Klein, and M. F. Schneider. 1988. Calcium dependence of inactivation of calcium release from the sarcoplasmic reticulum in frog skeletal muscle. *Biophysical Journal.* 53:602*a*. (Abstr.)

Simon, B. J., and M. F. Schneider. 1988. Time course of activation of calcium release from sarcoplasmic reticulum in skeletal muscle. *Biophysical Journal.* 54:1159–1163.

Smith, J. S., R. Coronado, and G. Meissner. 1986. Single channel measurements of the calcium release channel from skeletal muscle sarcoplasmic reticulum. Activation by Ca^{2+} and ATP and modulation by Mg^{2+}. *Journal of General Physiology.* 88:573–588.

Smith, J. S., T. Imagawa, J. Ma, M. Fill, K. P. Campbell, and R. Coronado. 1988. Purified ryanodine receptor from rabbit skeletal muscle is the calcium-release channel of sarcoplasmic reticulum. *Journal of General Physiology.* 92:1–26.